Drier winters drove Cenozoic open habitat expansion in North America

Tyler Kukla[1,1], Jeremy Caves Rugenstein[2,2], Daniel Enrique Ibarra[3,3], Matthew Winnick[4,4], Caroline AE Strömberg[5,5], and Page Chamberlain[1,1]

[1]Stanford University
[2]Colorado State University
[3]Brown University
[4]University of Massachusetts Amherst
[5]Department of Biology and Burke Museum of Natural History and Culture, University of Washington

November 30, 2022

Abstract

The shift from denser forests to open, grass-dominated vegetation in west-central North America between 26 and 15 million years ago is a major ecological transition with no clear driving force. This open habitat transition (OHT) is considered by some to be evidence for drier summers, more seasonal precipitation, or a cooler climate, but others have proposed that wetter conditions and/or warming initiated the OHT. Here, we use published (n=2065) and new (n=173) oxygen isotope measurements (δ18O) in authigenic clays and soil carbonates to test the hypothesis that the OHT is linked to increasing wintertime aridity. Oxygen isotope ratios in meteoric water (δ18Op) vary seasonally, and clays and carbonates often form at different times of the year. Therefore, a change in precipitation seasonality can be recorded differently in each mineral. We find that oxygen isotope ratios of clay minerals increase across the OHT while carbonate oxygen isotope ratios show no change or decrease. This result cannot be explained solely by changes in global temperature or a shift to drier summers. Instead, it is consistent with a decrease in winter precipitation that increases annual mean δ18Op (and clay δ18O) but has a smaller or negligible effect on soil carbonates that primarily form in warmer months. We suggest that forest communities in west-central North America were adapted to a wet-winter precipitation regime for most of the Cenozoic, and they subsequently struggled to meet water demands when winters became drier, resulting in the observed open habitat expansion.

Drier winters drove Cenozoic open habitat expansion in North America

T. Kukla[1], J. K. C. Rugenstein[2], D. E. Ibarra[3,4], M. J. Winnick[5], C. A. E. Strömberg[6], C. P. Chamberlain[1]

[1]Department of Geological Sciences, Stanford University, Stanford, CA 94305
[2]Department of Geosciences, Colorado State University, Fort Collins 80521
[3]Institute at Brown for Environment and Society and the Department of Earth, Environmental and Planetary Science, Brown University, Providence, RI 02912
[4]Department of Earth and Planetary Science, University of California, Berkeley, Berkeley, CA 94709
[5]Department of Geosciences, University of Massachusetts, Amherst, Amherst, MA 01003
[6]Department of Biology & Burke Museum of Natural History and Culture, University of Washington, Seattle, WA 98195

Key Points:

- Coupled clay-carbonate oxygen isotopes constrain paleo-precipitation seasonality in western North America.
- The west-east winter-wet to summer-wet climate gradient in North America was established by the Eocene.
- Oligocene-Miocene expansion of grassy, open habitats corresponded with drier winters.

Corresponding author: T. Kukla, tykukla@stanford.edu

Abstract

The shift from denser forests to open, grass-dominated vegetation in west-central North America between 26 and 15 million years ago is a major ecological transition with no clear driving force. This open habitat transition (OHT) is considered by some to be evidence for drier summers, more seasonal precipitation, or a cooler climate, but others have proposed that wetter conditions and/or warming initiated the OHT. Here, we use published (n=2065) and new (n=173) oxygen isotope measurements ($\delta^{18}O$) in authigenic clays and soil carbonates to test the hypothesis that the OHT is linked to increasing wintertime aridity. Oxygen isotope ratios in meteoric water ($\delta^{18}O_p$) vary seasonally, and clays and carbonates often form at different times of the year. Therefore, a change in precipitation seasonality can be recorded differently in each mineral. We find that oxygen isotope ratios of clay minerals increase across the OHT while carbonate oxygen isotope ratios show no change or decrease. This result cannot be explained solely by changes in global temperature or a shift to drier summers. Instead, it is consistent with a decrease in winter precipitation that increases annual mean $\delta^{18}O_p$ (and clay $\delta^{18}O$) but has a smaller or negligible effect on soil carbonates that primarily form in warmer months. We suggest that forest communities in west-central North America were adapted to a wet-winter precipitation regime for most of the Cenozoic, and they subsequently struggled to meet water demands when winters became drier, resulting in the observed open habitat expansion.

Plain Language Summary

The open habitat transition in west-central North America, about 26-15 million years ago, marks a widespread shift from closed forests to open woodlands, grasslands, and scrublands. This change favored mammals adapted to open habitats and laid the foundation for modern ecosystems. Despite this pronounced signal in floral and faunal communities pointing convincingly to a drier climate, widespread geochemical paleoclimate evidence for aridity is lacking. Our analysis of oxygen isotopes of soil carbonates and clays shows that this ecological regime shift co-occurs with a decline in winter precipitation leading to increased aridity across west-central North America.

1 Introduction

Between ∼26 and 15 million years ago, lowland forests spanning interior western and central North America (WCNA; 40-47°N; −123-−100°E; Fig. 1a) were largely replaced by open, grass-dominated habitats (Hunt, 1990; Webb & Opdyke, 1995; Wing, 1998; Strömberg, 2005; Harris et al., 2017). This is referred to as the open habitat transition (OHT), and it set the stage for the development of open woodland, grassland, and scrubland habitats that dominate much of WCNA today. Hypotheses for what drove the OHT invoke factors such as grassland-grazer interactions (Retallack, 2004b, 2013), global warming (Strömberg, 2005, 2011), and a combination of global cooling, increasing aridity and a shift to drier summers (Webb & Opdyke, 1995; Wing, 1998; Retallack, 2001, 2004b; Harris et al., 2017). However, evidence supporting these hypotheses often comes from the floral record itself (Webb & Opdyke, 1995; Wing, 1998; Retallack, 2004b; Strömberg, 2005), and there is limited independent data to test possible causes of the OHT.

Though vegetation reconstructions point to changes in temperature or precipitation across the OHT, the direction of change remains debated. Pooid grasses that expanded during the OHT are generally adapted to cooler conditions, but the survival of frost-intolerant taxa, including palms, suggests that warming with a transient cool episode (< 1 million years) may have triggered the OHT (Strömberg, 2005, 2011). Drier conditions across the OHT are supported by the expansion of open, grassy vegetation dominated by dry-adapted pooids (Wolfe, 1985; Webb & Opdyke, 1995; Wing, 1998; Strömberg, 2005; Harris et al., 2017), but the survival of moisture-dependent taxa suggests that any aridification was minimal (Strömberg, 2005, 2011). Instead, increased seasonal aridity (as opposed to annual) may explain the survival of moisture-dependent taxa during grassland expansion (Harris et al., 2017). Increasingly dry summers are supported by the OHT expansion of open woodland and savanna habitats presumed to be adapted to a warm dry season (Wolfe, 1985; Webb & Opdyke, 1995; Wing, 1998). Further, the shift from calcite to silica-rich paleosols in central Oregon across the OHT has been interpreted as showing a transition from summer-wet to winter-wet seasonality (Retallack, 2004b), but the link between precipitation seasonality and soil calcite/silica content remains tenuous. Additional, independent (non-floral) evidence for summer aridity is not available.

The modern relationship between vegetation and precipitation, however, suggests that wintertime moisture has a far greater influence on vegetation than the magnitude of summertime aridity (Clow, 2010; Hu et al., 2010; Trujillo et al., 2012; Knowles et al., 2017, 2018). The balance between winter precipitation supply (mostly snowpack) and spring/summer evaporative demand is closely correlated with gross primary productivity (GPP) in the western US (Hu et al., 2010; Knowles et al., 2018). Moreover, water isotope studies show that trees in mid-latitude North American and European forests generally use more winter moisture than summer during the growing season (Hu et al., 2010; Allen et al., 2019; Berkelhammer et al., 2020). Summer precipitation can drive montane forest GPP (Berkelhammer et al., 2017), especially when winter snowpack is already high (Berkelhammer et al., 2020), but the spatial pattern of open versus closed habitats is more sensitive to annual precipitation (Schimel et al., 2002) which, for most of WCNA, is dominated by winter (SI Fig. S1). Today, wetter wintertime climates in WCNA are typically characterized by higher tree cover, consistent with wooded, closed habitats, whereas low winter precipitation yields grassland-dominated ecosystems characterized by low tree cover (Fig. 1d,e). If this relationship holds through time, then decreases in winter precipitation should lead to decreasing biomass and the expansion of open, grassy habitats.

Here, we test the hypothesis that drier winters—rather than drier summers—led to aridification across WCNA and prompted the expansion of grasslands and open habitats. Precipitation seasonality transitions from winter-wet to summer-wet from west to east across WCNA today (Fig. 1c,d), so testing this hypothesis requires data that cover the OHT in time and space. Oxygen isotopes in precipitation ($\delta^{18}O_p$; ‰) derived from proxy records can be used to address this hypothesis because $\delta^{18}O_p$ is sensitive to seasonality and aridity (Salati et al., 1979; Dansgaard, 1964; Mix et al., 2013; Chamberlain et al., 2014; Winnick et al., 2014; Kukla et al., 2019) and $\delta^{18}O$ proxy coverage across WCNA is temporally comparable to, and often co-located with, paleobotanical archives (Fig. 1a). Oxygen isotopes are particularly useful because, while precipitation seasonality changes from west to east (Fig. 1c,d), the seasonality of $\delta^{18}O_p$ does not. Precipitation $\delta^{18}O$ is higher in the summer and lower in the winter across the entire WCNA (a correlation known as the "temperature effect" (Dansgaard, 1964); Fig. 1b). Thus, a change in the relative contribution of winter versus summer moisture would likely be accompanied by the same direction of change in $\delta^{18}O_p$ across WCNA.

We compare oxygen isotopes of two independent proxy materials—authigenic clay and soil carbonate—to reconstruct past precipitation seasonality. Soil carbonates can form on seasonal (and shorter) timescales, preserving seasonally biased oxygen isotope signals (Breecker et al., 2009; Peters et al., 2013; Gallagher & Sheldon, 2016; Huth et al., 2019; Kelson et al., 2020). The timing of soil carbonate formation is strongly influenced by precipitation seasonality with winter-wet (summer-wet) climates generally favoring carbonate formation in the summertime (spring/fall) when soil CO_2 and moisture are declining (Peters et al., 2013; Gallagher & Sheldon, 2016; Huth et al., 2019; Kelson et al., 2020). Clay minerals, in contrast, form on much longer timescales making them less likely to record a seasonal bias (Palandri & Kharaka, 2004; White et al., 2008; Maher et al., 2009), and are usually interpreted to reflect precipitation-weighted oxygen isotope ratios (Lawrence & Taylor, 1971; Stern et al., 1997; Tabor et al., 2002; Mix & Cham-

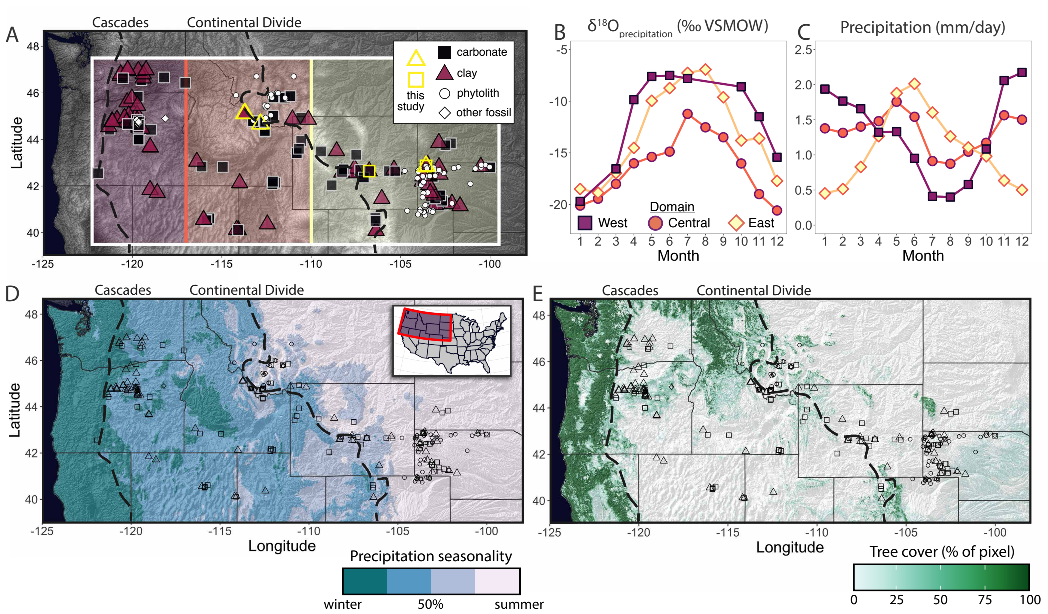

Figure 1. (**A**) Stable isotope and floral reconstruction sites with three domains denoted by rectangles (west=purple; central=orange; east=yellow). Elevation data (grayscale) were collected with the elevatR package in R (Hollister et al., 2021). (**B**) Modern average monthly $\delta^{18}O_p$ (data from the Waterisotopes Database (Database, 2019); note some months with no data in western domain) and (**C**) precipitation (data from PRISM (2012)) in each domain. (**D**) Modern precipitation seasonality (DJF / (DJF + JJA)) (data from PRISM (2012)) and (**E**) Tree cover (percent of pixel) (data from Geospatial Information Authority of Japan et al. (2016)). Dashed lines on maps denote Cascades Range ridgeline and the continental divide. Maps cover the geographic range of the purple box in the inset of panel D.

berlain, 2014; Gao et al., 2021). Since clays are more likely to record wet season $\delta^{18}O_p$ than carbonates, the difference between clay and carbonate $\delta^{18}O$ depends on (1) how much total precipitation falls in the wet season (the magnitude of seasonality) and (2) whether the wet season is the high-$\delta^{18}O$ or low-$\delta^{18}O$ season (*i.e.* summer or winter in WCNA, respectively).

We compile 2065 existing clay (n=235) and carbonate (n=1830) $\delta^{18}O$ measurements and present 173 new measurements (33 clay; 140 carbonate) spanning 162 sites across WCNA to assess precipitation seasonality on a regional scale (Amundson et al., 1996; Chamberlain et al., 2012; Fan et al., 2014, 2018; Fox & Koch, 2003, 2004; Horton et al., 2004; Kent-Corson et al., 2006, 2010; Kukla et al., 2021; McLean & Bershaw, 2021; Methner, Fiebig, et al., 2016; Methner, 2015; Mix & Chamberlain, 2014; Mix et al., 2013; Mulch et al., 2015; Mullin, 2010; Retallack, Wynn, & Fremd, 2004; Schwartz, 2015; Schwartz et al., 2019; Sjostrom et al., 2006; Takeuchi, 2007; Takeuchi & Larson, 2005; Takeuchi et al., 2010). These data reveal a diverging trend in clay and carbonate $\delta^{18}O$ across the OHT. We identify this trend in three domains across WCNA: (1) a western domain comprised of data west of the Rockies, (2) a central domain in the Rocky Mountain interior; and (3) an eastern domain including the eastern flank of the Rockies and the High Plains (see Fig. 1a-c). These three domains represent distinct regions of topography and precipitation seasonality and similar delineations have been previously used (Strömberg, 2005; Kohn & Fremd, 2007; Badgley & Finarelli, 2013; Kent-Corson et al., 2013; Badgley et al., 2017). Below, we argue that drier winters, not summers, are the most likely explanation for these diverging clay and carbonate $\delta^{18}O$ trends and we discuss implications for the expansion of open, grassy habitats during the OHT.

2 Methods

2.1 New paleosol carbonate and authigenic clay data

Our new data help fill key spatial and temporal gaps in the west to east transect. The data comprise 173 samples spanning the Salmon Basin in eastern Idaho (Harrison, 1985; Janecke & Blankenau, 2003; Schwartz et al., 2019), the Muddy Creek Basin in southwestern Montana (Dunlap, 1982; Janecke et al., 1999; Schwartz et al., 2019), the Flagstaff Rim region of Wyoming (Emry, 1973, 1992; Evernden et al., 1964), and the Toadstool Park region of northwestern Nebraska (Terry, 2001; Zanazzi et al., 2007). Salmon Basin data include 21 authigenic clay samples spanning the middle-late Oligocene following the stratigraphy of Harrison (1985) and the age constraints compiled in Schwartz et al. (2019) (M'Gonigle & Dalrymple, 1993; Axelrod, 1998). We did not find any soil carbonates of middle-late Oligocene age in the Salmon Basin, perhaps due to wetter conditions inhibiting carbonate formation. Muddy Creek Basin data span the Eocene and include both clay (n=4) and carbonate (n=29) samples pinned to the straigraphy of Dunlap (1982) with age constraints from Janecke et al. (1999). Most of the samples collected in the Muddy Creek Basin come from paleosols containing coeval gypsum indicative of evaporative conditions. Flagstaff Rim samples are all carbonates (n=30) that span the late Eocene and are linked to the stratigraphy of Emry (1992) and the compiled age constraints therein (Evernden et al., 1964; Swisher & Prothero, 1990). Toadstool Park data cover the late Eocene-early Oligocene with both clay (n=4) and carbonate (n=59 data). Our Toadstool samples are pinned to the stratigraphy of Terry (2001) following the age model of Zanazzi et al. (2007).

2.2 Carbonate stable isotopes

Carbonate samples collected as part of this study (n=140) were powdered using mortar and pestle or a handheld drill. Stable carbon and oxygen isotopes were measured at the Stanford University Stable Isotope Biogeochemistry Laboratory using a Thermo Finnigan Gasbench peripheral preparation system with isotope ratios measured in continuous flow (Thermo Finnigan ConFlo III) on a Finnegan MAT Delta+ XL mass spectrometer. Based on carbonate content 250 to 800 µg of sample powder were reacted with 0.25 ml of 105% phosphoric acid for 1 hour at 72 °C. External precision (1 sigma) of oxygen and isotope data was ±0.1‰ based on repeat measurements of internal carbonate standards that have been calibrated against NBS-18, NBS-19, and LSVEC. We report all $\delta^{18}O$ values relative to VSMOW.

2.3 Clay stable isotopes

Stable oxygen isotopes of authigenic clay minerals collected as part of this study (n=33) were measured at the Stanford University Stable Isotope Biogeochemistry Laboratory. About 250 g of bulk rock sample was suspended in DI water and the $< 0.5\mu m$ size fraction was separated out via a Thermo IEC centrifuge. The $< 0.5\mu m$ fraction was subsequently sequentially cleaned to remove contaminants: (1) 0.5 mol/L sodium acetate buffer solution to remove carbonates when necessary (Savin & Epstein, 1970); (2) 3% hydrogen peroxide solution to remove organic matter; and (3) ammonium citrate/sodium dithionite solution (80°C) to remove iron oxyhydroxides (Bird et al., 1993; Stern et al., 1997). Samples were then rinsed 5 times with deionized water and dried in oven at 60°C for at least 40 hours. Clay mineralogy was assessed via X-ray diffraction at the Environmental Measurements Facility at Stanford University. Analyses were conducted using a Rigaku MiniFlex 600 Benchtop X-ray Diffraction System equipped with a Cu anode set at the maximum power of 600W. Measurements were repeated after glycolation with one centimeter of ethylene glycol at the base of a sealed desiccator left overnight in an oven set to 65° C (Poppe et al., 2001). Mineral identification was determined with the Rigaku PDXL software and the USGS X-ray Diffraction Lab manual (Poppe et al., 2001). Samples contained predominantly smectite with minor contributions of quartz (SI Fig. S2). To prepare for isotope analyses clay samples were mixed with LiF and pressed into pellets. Samples were dried at 80°C in a vacuum oven prior to analysis.

Oxygen isotopic composition was determined using a laser fluorination line and measured on a Thermo Finnigan MAT 252 mass spectrometer in a dual inlet configuration (*e.g.* Sharp (1990); Sjostrom et al. (2006); Mix and Chamberlain (2014); Mix et al. (2016)). Prior to laser fluorination samples were exposed to three BrF_5 prefluourinations at 30 millitorr and then fluorinated using a New Wave Research MIR 10-25 infrared CO_2 laser in a 130 millitor BrF_5 atmosphere. Oxygen gas (O_2) was purified through liquid nitrogen cold traps and heated KBr trap prior to being frozen on a 5Å mol sieve (zeolite) prior to equilibration of the purified O_2 with the sample bellows. Measurements were made at a 2V intensity on mass $^{32}O_2$ and were standardized by measurements of NBS-28 quartz and bracketing using in-house smectite standard DS069, run in between samples to assess for drift. The external reproducibility was assessed based on corrected values of NBS-28 and the DS069 standard, giving values of ± 0.1‰ for each standard. Isotopic ratios are reported relative to Vienna Standard Mean Ocean Water (VSMOW).

2.4 Phytolith data compilation

Among paleobotanical sources of evidence, phytoliths stand out for providing information that is relevant for reconstructing the spread of open, grass-dominated habitats (Strömberg et al., 2018). Specifically, phytolith assemblages have been shown to reliably reflect the composition and dominance of grass communities in past vegetation on local to regional scales, as demonstrated by a body of modern analog work (*e.g.* Barboni et al. (2007); Iriarte and Paz (2009); Novello et al. (2012); Crifò and Strömberg (2020, 2021)). We therefore limited our compilation of paleovegetation data to phytolith studies and use these to define the OHT.

Phytolith-based data on the relative abundance of open-habitat grasses in the Cenozoic of Western North America were collected from the literature (SI Data; Strömberg (2005); Strömberg and McInerney (2011); Miller et al. (2012); Harris et al. (2017); Cotton et al. (2012); Chen et al. (2015); Hyland et al. (2019)). The compilation includes 216 phytolith assemblages ranging from the middle Eocene (∼40 Ma) to the latest Miocene (∼5 Ma) from Montana, Idaho, Nebraska, Kansas, Colorado, and Wyoming. These studies employed phytolith-based plant functional groups (PFT) following Strömberg and McInerney (2011) and thereafter (see Strömberg et al. (2018)), namely: (1) forest indicator (FI TOT) forms found in palms, woody or herbaceous dicotyledons, conifers, ferns, and tropical monocotyledonous herbs in the Order Zingiberales; (2) grass silica short cell phytoliths (GSSCP), exclusively produced by grasses (Poaceae), which can be subdivided into morphotypes typical of closed-habitat grasses (CH; e.g., bambusoid and early-diverging grasses, such as Anomochlooideae) and open-habitat (OH) grasses in the Pooideae (POOID-D, which are nearly exclusively produced by Pooideae, and POOID-ND, which are produced by many grass lineages but are most abundantly and commonly found in the C_3 Pooideae) and PACMAD clade (PACMAD TOT; C_3 and C_4 grasses in the subfamilies Panicoideae, Aristidoideae, Chloridoideae, Micrairioideae, Arundinoideae, and Danthonioideae (Grass Phylogeny Working Group II, 2012)), but also contains forms that cannot (currently) be assigned to a specific grass PFT because they are widely produced, as well as GSSCP that cannot be identified because they are broken or obscured (OTHG); (3) morphotypes typical of certain plants often associated with wetlands (AQ), such as sedges and horsetails; and (4) non-diagnostic and unclassified forms (OTH). OTH contains both forms commonly or exclusively produced by grasses, but that are not suitable for indicating grass biomass (NDG), and forms that are found in such a broad range of plants they are non-diagnostic (NDO) (Strömberg & McInerney, 2011).

To assess the relative abundance of open-habitat grasses in plant communities, we focused on the relative abundance of open habitat (OH) grasses (OH = POOID-D + POOID-ND + PACMAD TOT) in the sum of all diagnostic phytoliths (FI TOT + all GSSCP). To account for the fact that OTHG undoubtedly contains some GSSCP attributable to open-habitat grasses (as opposed to, in effect, all being counted as closed-habitat grasses), we 'scaled' the relative abundance of OH GSSCP following (McInerney et al., 2011). Specifically, the proportion (%) OH in vegetation was calculated as % OH phytoliths out of GSSCP–OTHG scaled to the relative abundance of all GSSCP out of the diagnostic sum (FI TOT + GSSC). In doing so, we reasonably assumed that OTHG contains the same proportion of CH and OH phytoliths as does the sum of CH, POOID-D, POOID-ND, and PACMAD TOT GSSCP (see discussion in Strömberg and McInerney (2011); McInerney et al. (2011)). We inferred 95% confidence intervals (unconditional case, using the total count as the sample size) for the %OH phytoliths using a bootstrap routine in the statistical software R (R Team, 2021) (code available upon request). Note that in several Eocene-Oligocene samples from Montana/Idaho, GSSCP assemblages were dominated by forms that are reminiscent of morphotypes typical of open-habitat grasses; however, their exact affinity and ecology remains unclear (Strömberg, 2005; Retallack, 2004a). These assemblages are marked as transparent in Figure 2.

2.5 Isotope data compilation and study domain

We compile stable isotope data within WCNA spanning the last 50 million years and filter and process the data in three steps. Starting with 3400 data points (all of the compiled and new data), we first remove samples outside of our study domain (40-47° N; −123-−100° E) and filter for smectite, kaolinite, and calcite minerals, excluding lacustrine carbonates, yielding 2238 data points. Of the clay samples, only 5 are kaolinite (of 268) and the rest are smectite as determined by X-ray diffraction by the original authors. We also eliminate Quaternary data (the last 2.6 Myr) to avoid confounding signals with glacial-interglacial cyclicity (especially the Laurentide ice sheet) which are known to have changed both mean annual precipitation and the pattern of atmospheric circulation across the western U.S. (Amundson et al., 1996; Oster et al., 2015; Oerter et al., 2016). Second, following the original authors' interpretations, we eliminate data that (1) do not reflect a primary meteoric signal (n=61; 2.5% of all data, (this study) (Horton et al., 2004; Chamberlain et al., 2012; McLean & Bershaw, 2021)); (2) were updated in a later publication (n=5; 0.2%, (Kent-Corson et al., 2006)); or (3) record a transient isotope excursion such as a climate event that may not reflect long-term, background conditions (n=6; 0.2%, (Methner, Mulch, et al., 2016)). Of the samples determined to not reflect primary meteoric conditions, most (n=56) are from the Muddy Creek Basin data presented in this study where we sampled from strata with interlayered gypsum (indicative of strong evaporation) and $\delta^{18}O$ values are generally high (although the evaporative designation of samples depends solely on the presence of gypsum). Finally, we average sample replicates so there is a single isotope value for each sample, yielding a total of 1851 samples. Data for each data processing step and an R script to conduct all data processing and statistical analyses are in the Supporting Information.

To produce the time series in Fig. 2, oxygen isotope ratios are averaged by sampling site. Sampling sites are defined by distinct sampled sections as reported by the original authors or based on proximity of sample coordinates. Records that cover more than 2 million years and reveal a long-term trend were sub-sampled at 1 million year intervals so the trend is not averaged out. In the eastern domain, $\delta^{18}O$ is positively correlated with longitude (see Fig. 3) and we de-trend the data using a linear regression applied to all eastern domain clay and carbonate data. De-trending these data ensures that trends in the eastern domain data through time are not attributable to changes in sampling density across the domain.

Finally, we calculate the pre-OHT $\delta^{18}O$ value for each domain by taking the average $\delta^{18}O$ of all data prior to 26 Ma (the OHT spans ∼26-15 Ma). This pre-OHT value is subtracted out from each domain so the domains can be directly compared in the time series of Fig. 2. It was previously recognized that there are two sub-domains in the western domain clay $\delta^{18}O$ data due to local topographic effects in Oregon (Kukla et al., 2021) and we subtract a pre-OHT value for each Oregon sub-domain to account for the $\delta^{18}O$ offset between them. Each sub-domain records the ∼3‰ increase in clay $\delta^{18}O$ across the OHT (Kukla et al., 2021). The carbonate data in the west come from the same sub-domain, except for one data point (McLean & Bershaw, 2021) that we remove because it is insufficient to analyze trends through time.

2.6 The difference in clay and carbonate $\delta^{18}O$ ($\Delta\delta^{18}O_{clay-carb}$)

2.6.1 Theoretical background

The comparison of clay and carbonate $\delta^{18}O$ ($\Delta\delta^{18}O_{clay-carb}$) is useful for determining if clays and carbonates formed under the same conditions of temperature and water $\delta^{18}O$ (“co-equilibrium”). Starting with the fractionation equations for calcite carbonate (Kim & O’Neil, 1997) and clays (Sheppard & Gilg, 1996) we can derive the following equations to predict co-equilibrium $\Delta\delta^{18}O_{clay-carb}$ as a function of temperature (see SI Text S1 for derivation):

$$\Delta\delta^{18}O_{smectite-calcite} = 2.55(10^6T^{-2}) - 18.03(10^3T^{-1}) + 28.37 \tag{1}$$

$$\Delta\delta^{18}O_{kaolinite-calcite} = 2.76(10^6T^{-2}) - 18.03(10^3T^{-1}) + 25.67. \tag{2}$$

For the range of environmental temperatures, co-equilibrium $\Delta\delta^{18}O_{clay-carb}$ for smectite- and kaolinite-calcite is near −3.5‰ (± ∼ 0.3‰ depending on the temperature) (SI Fig. S3). Because the co-equilibrium $\Delta\delta^{18}O_{clay-carb}$ is not very sensitive to temperature, we can interpret $\Delta\delta^{18}O_{clay-carb}$ values near −3.5‰ as clays and carbonates likely forming under similar conditions regardless of the formation temperature.

However, previous work comparing clay and carbonate $\delta^{18}O$ has rarely found the minerals to be in co-equilibrium (Torres-Ruíz et al., 1994; Stern et al., 1997; Tabor et al., 2002; Poage & Chamberlain, 2002; Gao et al., 2021). Instead, $\Delta\delta^{18}O_{clay-carb}$ is consistently below −3.5‰ in places where the wet season is thought to be the low-$\delta^{18}O$ season (Stern et al., 1997; Tabor et al., 2002) and above −3.5‰ when the wet season is the high-$\delta^{18}O$ season (Poage & Chamberlain, 2002; Gao et al., 2021). These findings are consistent with soil carbonates forming outside of the wet season (Breecker et al., 2009; Peters et al., 2013; Kelson et al., 2020; Huth et al., 2019; Gallagher & Sheldon, 2016) and clays forming more slowly (Palandri & Kharaka, 2004; White et al., 2008; Maher et al., 2009) capturing precipitation-weighted conditions (Lawrence & Taylor, 1971). Soil carbonates are also known for predominantly forming in warm months, and some studies have found that seasonal biases in carbonate formation (determined via clumped isotope thermometry) do not necessarily correspond to the same seasonal bias in carbonate $\delta^{18}O$ (*e.g.* Kelson et al., 2020). We consider the implications of carbonate $\delta^{18}O$ and formation biases differing in the discussion. Differences in mineral formation temperature can also affect $\Delta\delta^{18}O_{clay-carb}$, but $\Delta\delta^{18}O_{clay-carb}$ is about three times more sensitive to $\delta^{18}O_p$ seasonality than temperature seasonality (SI Fig. S4). Taken together, since WCNA $\delta^{18}O_p$ is higher in the summer and lower in the winter, we expect $\Delta\delta^{18}O_{clay-carb}$ to be higher in a summer-wet climate, and lower in a winter-wet climate. While this basic theoretical framework is supported by independent clay (Lawrence & Taylor, 1971) and soil carbonate studies (Peters et al., 2013; Gallagher & Sheldon, 2016; Kelson et al., 2020), we are not aware of any modern work directly comparing clay and carbonate $\delta^{18}O$.

2.6.2 Calculating the clay-carbonate $\delta^{18}O$ difference from data

In order to quantify $\Delta\delta^{18}O_{clay-carb}$ in each domain at each timeslice we conduct a two-sample Student's t-test (using the t.test function in R version 4.0.2) comparing clay and carbonate $\delta^{18}O$ for each designation (west, central, east; pre-OHT, post-OHT). Pre-OHT and post-OHT are defined as all data before 26 Ma and after 15 Ma, respectively. We exclude data within the OHT in order to unambiguously compare pre- and post-OHT conditions, recognizing that the precise timing of the transition and whether it occurred synchronously or asynchronously across WCNA remains uncertain. The t-test returns the difference in clay and carbonate $\delta^{18}O$ means and the 95% confidence interval around this difference. For the eastern domain, the data were de-trended using the same regression line noted in section 2.5. For the western domain we do not consider clay or carbonate $\delta^{18}O$ from the sub-domain that has only one carbonate value (see section 2.5). We test whether $\Delta\delta^{18}O_{clay-carb}$ changes significantly ($p < 0.05$; null hypothesis that $\Delta\delta^{18}O_{clay-carb}$ does not change) in each domain from pre- to post-OHT using a two-way analysis of variance test (ANOVA) in R (the glm function, R version 4.0.2).

In order to further validate our $\Delta\delta^{18}O_{clay-carb}$ results, we repeat the above analysis for the mean $\delta^{18}O$ at each sample site, rather than each individual measured sample (SI Fig. S5). If the site-averages give similar results for each domain, we can be confident that our results are not biased by sites with more samples. The p-value for the change in $\Delta\delta^{18}O_{clay-carb}$ in the site-average analysis is below 0.05 in each domain. Site averages also yield similar $\Delta\delta^{18}O_{clay-carb}$ results as individual samples. Therefore, we do not find any evidence that our data are biased by densely sampled sites.

3 Results

3.1 Oxygen isotope and vegetation data through time

We first compare trends in phytolith (plant biogenic silica) and isotope data across WCNA through time (Fig. 2). Phytolith data coverage is restricted to the central and eastern domains (existing data to the west and south are outside the bounds of isotope data for comparison (40-47°N; -123--100°E; Fig. 1) (*e.g.* Dillhoff et al. (2014); Smiley et al. (2018); Loughney et al. (2020)). However, the open habitat transition has also been identified in the western domain from fossil megafloras and paleosol morphology and these sites are noted by "other fossil" in Figure 1a (Retallack, 2004b; Retallack, Orr, et al., 2004; Retallack, 2004a). Figure 2c shows the percent of phytoliths that indicate open habitat conditions in an updated WCNA phytolith compilation. The percent of open habitat phytoliths (and the percent of grass phytoliths; SI Fig. S6) increases between 26 and 15 Ma from $\sim$20% to $\sim$73%, defining the open habitat transition. Since the major trends in the proxy data occur across the OHT, not before or after, we directly compare pre- and post-OHT oxygen isotope data in the next section to quantify their relative differences.

Authigenic carbonate $\delta^{18}O$ data vary by more than 10‰ with no uniform trends across the OHT (Fig. 2b and adjacent box plot). Clay $\delta^{18}O$, in contrast, increases by $\sim$1-3‰ across the OHT in each domain (Fig. 2a). The increase in clay $\delta^{18}O$ is statistically significant ($p<0.05$) in the full and site averaged datasets in the western and central domains whereas, in the east, it is significant in the site averaged data ($p=0.03$) and just above the significance level with the full dataset ($p=0.08$). We therefore consider each increase in clay $\delta^{18}O$ to be significant. In contrast, when considering the full and site averaged carbonate data there is no significant change in the western and central domains and a significant decrease in $\delta^{18}O$ in the east (see SI Table S1). Carbonate $\delta^{18}O$ increases significantly in the western domain in the full dataset, but this increase is not

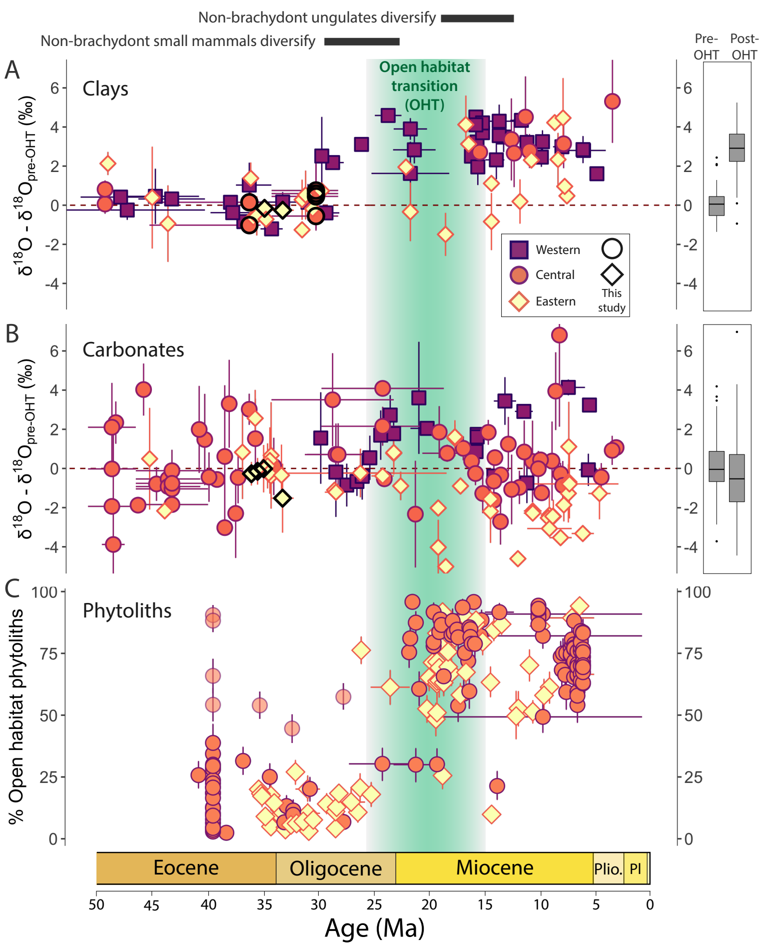

Figure 2. Cenozoic time series of $\delta^{18}O$ data relative to pre-OHT $\delta^{18}O$ for the western (purple squares), central (orange circles), and eastern (yellow diamonds) domain (**A**) authigenic clay and (**B**) soil carbonate isotope records. Points outlined in black are new data. Box plots to the right of (A) and (B) show pre- and post-OHT distributions. (**C**) Percent of open habitat phytoliths based on morphology. The increase in open habitat percent defines the OHT. Slightly transparent points mark samples where grass phytolith assemblages were dominated by forms produced by (likely) open-habitat grasses of unknown affinity (Strömberg, 2005; Miller et al., 2012). The OHT has also been identified in the western domain with different methods (*e.g.* Retallack (2004b); Retallack, Orr, et al. (2004); Retallack (2004a); Wheeler et al. (2006))

significant in the site averaged data, suggesting the signal is driven by a small number of densely sampled sites or site averaged data coverage is insufficient to resolve the signal. We note that the carbonate $\delta^{18}O$ record in the western domain does not start until just prior to the OHT due to absence of soil carbonates in paleosol strata (Bestland et al., 1997, 2002). In general, the first soil carbonates to form in the western domain show features similar to groundwater carbonates, rather than nodules forming well within the vadose zone (Methner, Fiebig, et al., 2016) (SI Text S2, SI Fig. S7).

3.2 Oxygen isotopes of clay and carbonate by geographic domain

Clay and carbonate $\delta^{18}O$ generally decrease from the western to central domain, then increase through the eastern domain. This longitudinal pattern is similar to that of modern meteoric and surface water $\delta^{18}O$ (SI Fig. S8), which reflects the balance between westerly rainout in the west and central domains, and increasing mixing with warm season, Gulf of Mexico moisture to the east (Kendall & Coplen, 2001; Z. Liu et al., 2010).

This spatial pattern of clay and carbonate $\delta^{18}O$ is similar before and after the OHT, but the offset between clay and carbonate $\delta^{18}O$ ($\Delta\delta^{18}O_{clay-carb}$; ‰) is not (Fig 3a,b). Within a given domain, clay and carbonate $\delta^{18}O$ approach more similar values ($\Delta\delta^{18}O_{clay-carb}$ closer to zero) after the OHT than before (Fig. 3c). In the central domain, clay and carbonate $\delta^{18}O$ are more similar after the OHT mostly due to an increase in clay $\delta^{18}O$ from ∼8-9‰ to ∼12-13‰. In the east, clay and carbonate $\delta^{18}O$ shift to nearly the same values after the OHT, especially east of −105 degrees longitude. Unlike the shift toward more similar clay/carbonate $\delta^{18}O$ in the west and central domains, the eastern domain shift is partly driven by lower carbonate $\delta^{18}O$ after the OHT.

We quantify $\Delta\delta^{18}O_{clay-carb}$ for each of the three domains before and after the OHT in Figure 3c. The dashed, red line denotes the expected $\Delta\delta^{18}O_{clay-carb}$ when clays and carbonates form in co-equilibrium ($\Delta\delta^{18}O_{clay-carb} \approx -3.5$). The $\Delta\delta^{18}O_{clay-carb}$ values show consistent spatial structure through time, with lower values in the west, intermediate values in the central domain, and higher values in the east both before and after the OHT. Across the OHT, $\Delta\delta^{18}O_{clay-carb}$ increases in each domain ($p<0.05$) with the largest increases in the central and eastern domains and a relatively muted increase in the west (Fig. 3c, SI Fig. S5).

In the western domain, the mean $\Delta\delta^{18}O_{clay-carb}$ is -7.2 ± 0.9‰ before the OHT and -5.6 ± 1.0‰ after (mean and 95% confidence interval). The clay-carbonate $\delta^{18}O$ difference before and after the OHT is largest in the central domain where $\Delta\delta^{18}O_{clay-carb}$ is -5.6 ± 0.5‰ before and -2.2 ± 0.7‰ after. And in the east, $\Delta\delta^{18}O_{clay-carb}$ increases from -2.9 ± 0.4‰ to -0.2 ± 1.0‰ across the OHT. The increase in $\Delta\delta^{18}O_{clay-carb}$ in the three domains ranges from 1.6-3.3‰ with an average increase of 2.6‰.

4 Discussion

4.1 Clay and carbonate oxygen isotope trends across the OHT

Previous work speculated that the increase in western domain clay $\delta^{18}O$ across the OHT can be explained by a greater fraction of annual precipitation occurring in summer, perhaps due to Cascades Range uplift disproportionately blocking winter moisture compared to summer (Kukla et al., 2021). A disproportionate decrease in winter precipitation could also explain the increase in clay $\delta^{18}O$ in the central and eastern domains. However, a gap in our central domain data across the OHT prohibits a direct link to the western domain data. Additionally, if the eastern domain increase in clay $\delta^{18}O$ (and decrease in carbonate $\delta^{18}O$) is driven by less winter precipitation, the causal mechanism may differ from the western domain since the $\delta^{18}O$ shift appears delayed (Fig. 2a) (we return to this point in Section 4.3).

The increase in clay $\delta^{18}O$, by itself, is not compelling evidence for a change in the seasonality of precipitation. Many other factors could drive the same isotopic trend, including an increase in $\delta^{18}O_p$ driven by warmer temperatures (Dansgaard, 1964), an increase in clay-water isotopic fractionation driven by cooler temperatures (Sheppard & Gilg, 1996), greater soil evaporation or evaporation of falling raindrops (Barnes & Allison, 1983; Zimmermann et al., 1967; Lee & Fung, 2008), and more upwind recycling of moisture back into the atmosphere (Chamberlain et al., 2014; Kukla et al., 2019; Salati et al., 1979; Winnick et al., 2014; Mix et al., 2013). However, global climate both warmed

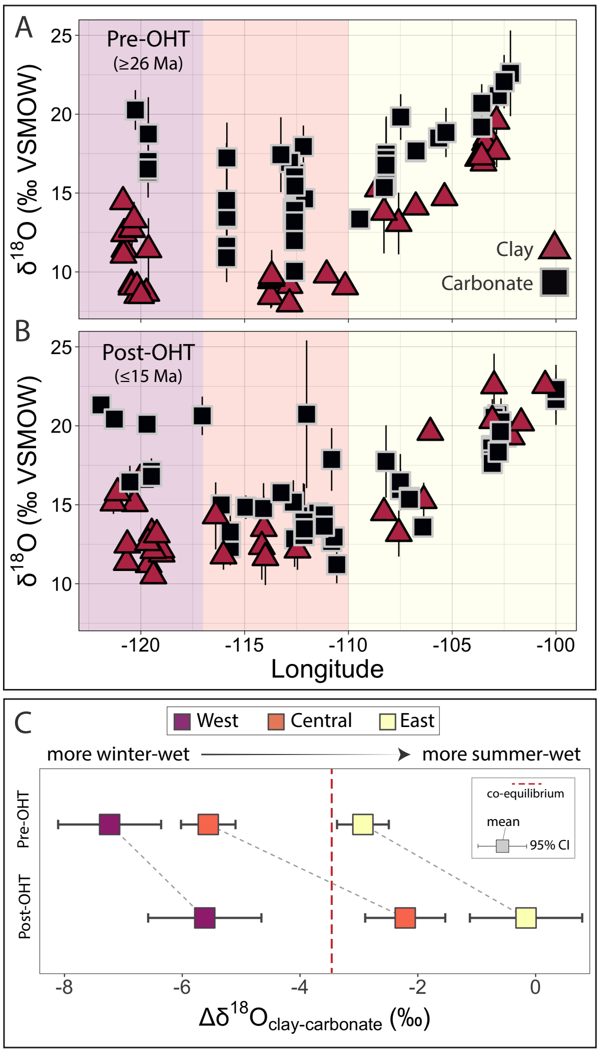

Figure 3. Longitudinal profiles of site-averaged authigenic clay (red triangles) and soil carbonate (dark purple squares) $\delta^{18}O$ (**A**) before the OHT and (**B**) after the OHT. Background rectangle color corresponds to domain (west=purple; central=orange; east=yellow). (**C**) The difference in clay and carbonate $\delta^{18}O$ ($\Delta\delta^{18}O_{clay-carb}$) before (upper) and after (lower) the OHT in the western (purple), central (orange) and eastern (yellow) domains. Red, dashed line is the $\Delta\delta^{18}O_{clay-carb}$ co-equilibrium value of -3.5‰.

and cooled across the OHT (Zachos et al., 2001; Westerhold et al., 2020), so temperature is unlikely to explain the unidirectional $\delta^{18}O$ increase. Soil and post-condensation evaporation can increase with drying, but the isotopic effect would likely be stronger in soil carbonates than clays because evaporation is highest in warmer months when soil carbonates tend to form. This is inconsistent with our finding that the main $\delta^{18}O$ increase occurs in clays, while carbonate $\delta^{18}O$ stays the same or decreases. Finally, upwind moisture recycling has little effect on $\delta^{18}O_p$ at sites close to the coast where there is minimal upwind land area for recycling to occur, such as in the western domain (Chamberlain et al., 2012; Kukla et al., 2019, 2021). Thus, it is unlikely that upwind recycling could drive a $\delta^{18}O$ increase in all three domains. We also note that there is no change in the mineralogy of clay samples across the $\delta^{18}O$ shift. Importantly, the mechanism for the increase in clay $\delta^{18}O$ must also be consistent with the carbonate $\delta^{18}O$ data, which either stay the same or decrease across the OHT. If clays and carbonates are generally recording the same information through time then we would not expect diverging $\delta^{18}O$ trends.

The lack of a corresponding increase in soil carbonate $\delta^{18}O$ supports the hypothesis that the clay $\delta^{18}O$ shift is driven by a decrease in winter precipitation. Mid-latitude soil carbonates should generally be less sensitive to changes in winter precipitation due to their strong bias to forming in warmer months, as supported by clumped isotope studies (*e.g.* Kelson et al., 2020). This delay between winter precipitation and warm season soil carbonate formation implies that soil carbonates either (1) form in contact with precipitation that falls in warmer months (higher $\delta^{18}O$) that is not influenced by changes in winter precipitation, or (2) carbonates form in contact with a combination of warm season precipitation and evaporating groundwater (which is often sourced from winter moisture) (Jasechko et al., 2014), such that summer precipitation dampens any winter signal (Quade et al., 1989). Indeed, late Quaternary soil carbonates in the western U.S. suggest that winter moisture can be incorporated in summer carbonate formation (Kelson et al., 2020), but the influence of winter moisture appears small except at the most winter-wet sites (SI Fig. S9) (Kelson et al., 2020). This result is consistent with clays being more sensitive to winter drying than carbonates, explaining why carbonate $\delta^{18}O$ does not show the same increase observed in the clay data.

The decrease in eastern domain carbonate $\delta^{18}O$ can also be explained by winter drying. Studies of modern (or latest Quaternary) soil carbonates have found that carbonates tend to form in the summer in more winter-wet conditions, and spring or fall in summer-wet conditions (*e.g.* Peters et al., 2013; Gallagher and Sheldon, 2016; Kelson et al., 2020). Wetter winter conditions prior to the OHT could have restricted soil carbonate formation to the warmest months of the year when $\delta^{18}O_p$ is highest. Subsequent winter drying would lead to drier springtime soils, likely increasing carbonate formation in the spring when soil moisture $\delta^{18}O$ is lower due to a combination of lower precipitation $\delta^{18}O$ and less evaporatively enriched groundwater recently recharged by winter (low-$\delta^{18}O$) precipitation and snowmelt (*e.g.* Jasechko et al., 2014). We would not expect to see the same shift in the timing of carbonate formation in the central and western domains because these regions are more winter-wet today, indicating that drier winters across the OHT would not have established such a summer-wet climate as exists in the east. Indeed, the greater influence of summer moisture in the eastern domain can also explain the relatively muted increase in clay $\delta^{18}O$ compared to the central and western records (SI Table S1). If summer precipitation was already high in the east, drier winters would have a diminished effect on precipitation-weighted annual (and therefore clay) $\delta^{18}O$.

4.2 Precipitation seasonality before and after the OHT

The difference between clay and carbonate $\delta^{18}O$ ($\Delta\delta^{18}O_{clay-carb}$) before and after the OHT provides additional insight to the role of precipitation seasonality. If carbonates are generally less sensitive to winter drying than clays, then $\Delta\delta^{18}O_{clay-carb}$ will differ from the co-equilibrium value of ~ -3.5‰, especially in more winter-wet regions. Specifically, because winter is the low-$\delta^{18}O$ season in WCNA today, $\Delta\delta^{18}O_{clay-carb}$ will become more negative with a more winter-wet climate due to an amplified winter bias in clay $\delta^{18}O$ compared to carbonate. Alternatively, we expect $\Delta\delta^{18}O_{clay-carb}$ to increase in a less-winter wet (more summer-wet) climate. If summer is wet enough to restrict soil carbonate formation (and its oxygen isotope bias) to spring and fall conditions, as argued above, then $\Delta\delta^{18}O_{clay-carb}$ will increase and may exceed -3.5‰ due to a summer (high-$\delta^{18}O$) bias in clay $\delta^{18}O$ compared to carbonate. Ultimately, because the relative biases in clay and carbonate mineral formation and $\delta^{18}O$ depend on precipitation seasonality, changes in $\Delta\delta^{18}O_{clay-carb}$ can encode changes in the seasonal balance of precipitation in the past.

An implicit assumption in our analysis is that, like today, winter has been the low-$\delta^{18}O_p$ season across WCNA since the Paleogene (see Fig. 1b). Isotope-enabled climate models and oxygen isotope data from seasonal bivalves confirm that winter has been the low-$\delta^{18}O$ season since at least the early Eocene (∼50 Ma) (Norris et al., 1996; Morrill & Koch, 2002; Feng et al., 2013). Moreover, the atmospheric circulation patterns that set WCNA $\delta^{18}O$ seasonality—high-$\delta^{18}O$ convective precipitation during warm months and synoptic-scale, low-$\delta^{18}O$ precipitation during cold months (Feng et al., 2013; Z. Liu et al., 2010)—are robust in models, even in hot Eocene climates (Sewall & Sloan, 2006; Feng et al., 2013) and with much lower WCNA topography (Feng et al., 2013). Strong correspondence between west-east trends in paleo-proxy and modern $\delta^{18}O$ provides additional support that the basic circulation patterns are unchanged (SI Fig. S8). The seasonal $\delta^{18}O$ amplitude and baseline very likely changed in the past, but this does not violate our assumption.

By assuming winter was the low-$\delta^{18}O$ season throughout our record, we can infer precipitation seasonality from $\Delta\delta^{18}O_{clay-carb}$. As stated above, we interpret higher $\Delta\delta^{18}O_{clay-carb}$ values as consistent with a more summer-wet climate and lower $\Delta\delta^{18}O_{clay-carb}$ as more winter-wet (illustrated in Fig. 4a). In theory, the $\Delta\delta^{18}O_{clay-carb}$ co-equilibrium value of $-3.5‰$ represents the threshold between winter-wet and summer-wet climates in WCNA, but this has yet to be verified with data from modern (or late Quaternary) soils. When $\Delta\delta^{18}O_{clay-carb}$ is equal to the co-equilibrium value we can infer that (1) no season is wet enough to inhibit carbonate formation so clays and carbonates form at the same time of year; or (2) clays and carbonates form at different times of year but with the same mean $\delta^{18}O_p$ and temperature conditions. The latter is possible if, for example, clays form year-round while carbonate formation is restricted to the spring or fall with $\delta^{18}O_p$ and temperature approximating annual mean conditions.

We argue that the OHT coincides with a shift to drier winters that may mark the establishment of modern precipitation seasonality across WCNA. Increasing $\Delta\delta^{18}O_{clay-carb}$ after the OHT points to drier winters that increased the summertime (high-$\delta^{18}O_p$) fraction of annual precipitation (increasing clay $\delta^{18}O$) with a negligible effect on summer (and soil carbonate) $\delta^{18}O$ in the west and central domains and a counteracting effect on the timing of carbonate formation in the east. The increase in $\Delta\delta^{18}O_{clay-carb}$ occurs in all domains and, if $-3.5‰$ represents a winter-wet versus summer-wet threshold, would likely mark the onset of summer-wet conditions in the east. This spatial pattern of precipitation seasonality is similar to modern (although the central domain $\Delta\delta^{18}O_{clay-carb}$ is slightly higher than expected) , suggesting the modern gradient was established around the time that open, grassy habitats expanded.

Other mechanisms that can alter $\Delta\delta^{18}O_{clay-carb}$ are unlikely to explain our results. For example, an increase in winter $\delta^{18}O$ could explain a shift toward higher clay $\delta^{18}O$ in the west and central domains, but global cooling and Cascades uplift since the OHT (Zachos et al., 2001; Reiners et al., 2002; Kohn & Fremd, 2007; Takeuchi et al., 2010; Methner, Fiebig, et al., 2016; Bershaw et al., 2019; Pesek et al., 2020; Westerhold et al., 2020; McLean & Bershaw, 2021) should, all else being equal, decrease winter $\delta^{18}O$. Colder clay formation temperatures are also consistent with increasing clay $\delta^{18}O$ and $\Delta\delta^{18}O_{clay-carb}$, but any cooling would likely occur in the winter and summer, causing the same signal in soil carbonate $\delta^{18}O$. The OHT itself might decrease soil CO_2 by decreasing productivity, which can affect carbonate $\delta^{18}O$ by changing the seasonal timing of carbonate formation. However, if carbonate formation tracks the timing of peak photosynthesis and root water uptake (Meyer et al., 2014), we expect the OHT to shift soil carbonate to the summer, likely increasing carbonate $\delta^{18}O$ and decreasing, not increasing, $\Delta\delta^{18}O_{clay-carb}$, in conflict with our findings. Additionally, lower soil productivity should increase soil carbonate $\delta^{13}C$ by decreasing soil respiration (Caves et al., 2016; Rugenstein & Chamberlain, 2018; Licht et al., 2020), and this is not observed (SI Fig. S10).

Our results are also difficult to reconcile with the idea that carbonates and clays, although forming at different times of the year, are recording essentially the same wet season moisture (*e.g.* Torres-Ruíz et al. (1994); B. Liu et al. (1996); Stern et al. (1997)). If this moisture is unevaporated, $\Delta\delta^{18}O_{clay-carb}$ should stay close to the co-equilibrium value of -3.5‰, although it is more likely that carbonates would record some evaporative offset (^{18}O enrichment) of this moisture (Quade et al., 1989; Stern et al., 1997; Quade & Cerling, 1995). If this evaporative offset is constant over space relative to precipitation-weighted $\delta^{18}O_p$, then most $\Delta\delta^{18}O_{clay-carb}$ variations will be due to differences in mineral formation temperature (since clays and carbonates would effectively record the same source water), in which case $\Delta\delta^{18}O_{clay-carb}$ should be higher in winter-wet regions due to a relative cold bias in clay formation that increases clay $\delta^{18}O$. This would lead to $\Delta\delta^{18}O_{clay-carb}$ decreasing from west-to-east, which is not observed either before or after the OHT. Alternatively, a larger evaporative offset in winter-wet climates due to drier summers could reverse this effect by increasing carbonate $\delta^{18}O$ relative to clay and decreasing $\Delta\delta^{18}O_{clay-carb}$. However, this means the evaporative offset would have to decrease in each domain across the OHT in order to increase $\Delta\delta^{18}O_{clay-carb}$. Since carbonates would be forming in contact with this less-evaporated moisture, a decrease in summer evaporation would primarily affect carbonate, rather than clay $\delta^{18}O$, making this scenario is unlikely because the clay $\delta^{18}O$ data drive most of the WCNA $\Delta\delta^{18}O_{clay-carb}$ increase. Additionally, a decrease in the evaporative offset of $\delta^{18}O$ would make clay and carbonate formation waters more isotopically similar, likely shifting $\Delta\delta^{18}O_{clay-carb}$ closer to -3.5‰, yet $\Delta\delta^{18}O_{clay-carb}$ increases away from -3.5‰ in the eastern domain (the only site where carbonate $\delta^{18}O$ decreases). Thus, it is difficult to reconcile the spatial pattern of $\Delta\delta^{18}O_{clay-carb}$ and its increase across the OHT with a scenario where clays and carbonates are recording the same moisture source, even if there is some evaporative offset between the two minerals. We therefore conclude that our $\Delta\delta^{18}O_{clay-carb}$ results require relative seasonal source moisture biases between clays and carbonates.

Figure 4 presents a conceptual model for our results, linking $\Delta\delta^{18}O_{clay-carb}$ to precipitation seasonality (Fig. 4a) and mapping these seasonal trends on our WCNA domain (Fig. 4b). Based on the relationship between the average post-OHT $\Delta\delta^{18}O_{clay-carb}$ and modern precipitation seasonality (DJF/(JJA+DJF)) in each domain, the increase in $\Delta\delta^{18}O_{clay-carb}$ values is consistent with about a 25% decrease in the winter fraction of precipitation across the OHT (SI Fig. S11; Fig. 4b) (this analysis effectively assumes modern precipitation seasonality was established post-OHT). This approximation is crude, but it captures the winter precipitation trend and illustrates two useful points. First, the Cascades Range, which marks the boundary between very winter-wet and somewhat winter-wet climates (Fig. 4b) was likely a less effective barrier to the wintertime westerlies before the OHT (Fig. 4b). Second, summer precipitation accounted for a smaller fraction of annual precipitation before the OHT, precluding a summer-wet climate in Oregon prior to grassland expansion (Retallack, 2004b).

Our results are not compatible with the demise of a summer-wet climate in the western domain at the OHT (Retallack, 2004b), even when we ignore our assumption that winter has remained the low-$\delta^{18}O_p$ season. For example, in summer-wet "monsoon" climates summer is often the low-$\delta^{18}O_p$ season. If the OHT marks the demise of summer-wet conditions and low-$\delta^{18}O_p$ summers, then summer drying would shift the wet season from a low-$\delta^{18}O_p$ summer to a low-$\delta^{18}O_p$ winter. This effect would likely lead to no change or a decrease in clay $\delta^{18}O$ and possibly an increase in carbonate $\delta^{18}O$ (see SI Text S3), in conflict with our results. Changes in mineral formation temperatures might counteract these effects, but are unlikely to erase them because $\Delta\delta^{18}O_{clay-carb}$ is nearly $3x$ more sensitive to precipitation seasonality than to temperature seasonality (SI Fig. S4) and soil temperature seasonality is generally dampened relative to surface temperatures (Hillel, 1982; Gallagher et al., 2019). While we cannot unequivocally rule out temperature and summer precipitation change across the OHT, our results indicate that the largest climatic signal comes from a decrease in winter precipitation.

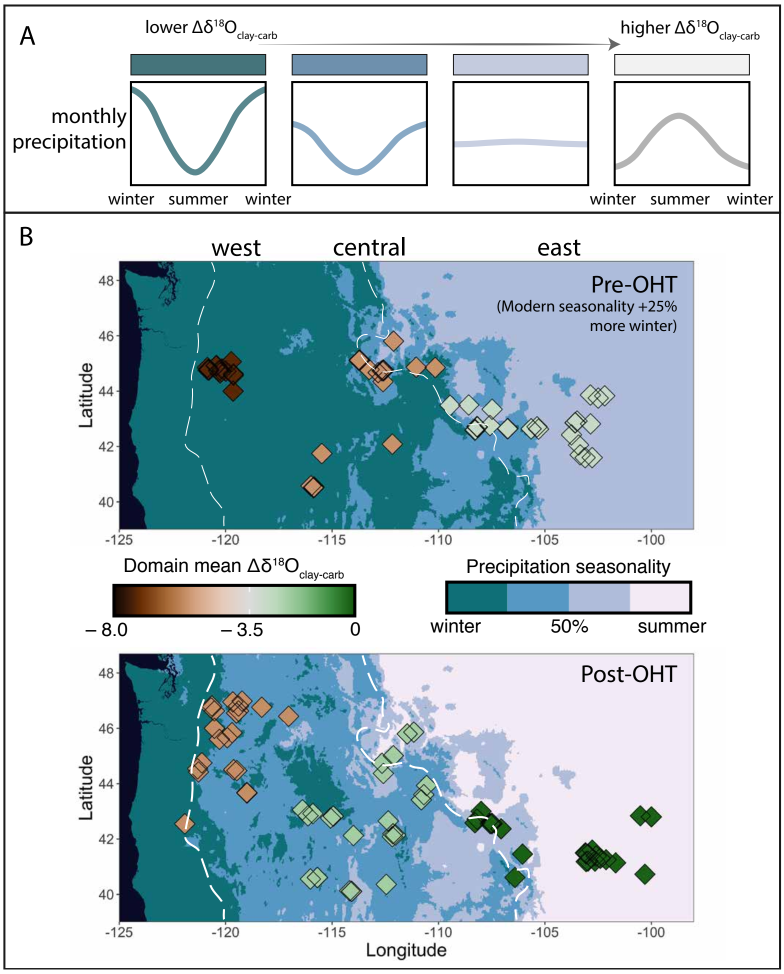

Figure 4. Conceptual model for WCNA precipitation seasonality. (**A**) $\Delta\delta^{18}O_{clay-carb}$ increases as precipitation seasonality shifts from winter-wet (left panel) to summer-wet (right panel). (**B**) An illustration of pre-OHT precipitation seasonality (top panel) inferred from the post-OHT $\Delta\delta^{18}O_{clay-carb}$-modern seasonality relationship (bottom panel). Data points are colored by the domain mean $\Delta\delta^{18}O_{clay-carb}$. Post-OHT western and central domain $\Delta\delta^{18}O_{clay-carb}$ approximates pre-OHT central and eastern domain values, respectively. Dashed white lines approximate the Cascades Range (left) and Continental Divide (right).

4.3 A mechanism for winter drying

While our analysis cannot confirm a cause for winter drying, it allows us to propose a testable hypothesis based on three observations. First, the isotope trends appear unidirectional (like the OHT itself), so the forcing may have been unidirectional, too. Second, topography is the main driver of the spatial pattern of modern precipitation seasonality today. The Cascades ridgeline divides very winter-wet from somewhat winter-wet climates, and the continental divide separates somewhat winter-wet from neutral or summer-wet climates (Lora & Ibarra, 2019) (Fig. 1). Third, the clay and carbonate $\delta^{18}O$ trends are not the same in each domain, and the eastern clay $\delta^{18}O$ increase lags behind the western domain. Based on these observations, we propose winters became drier due to tectonics—most likely the uplift of the Cascades Range.

Cascades uplift is a plausible driver of drier winters because it was (mostly) unidirectional and the Cascades mark a significant boundary in precipitation seasonality today (Fig. 4b). The Cascades block more winter precipitation than summer precipitation as they directly intercept winter westerly moisture (Siler et al., 2013; Siler & Durran, 2016; Rutz et al., 2014), and this seasonal difference in rainshadow strength is evident in oxygen isotopes of precipitation—$\delta^{18}O_p$ decreases more over the Cascades in the winter and less in the summer (Z. Liu et al., 2010). The seasonality of rainshadow strength means that, east of the Cascades, uplift will have two effects on annual mean $\delta^{18}O_p$ that act in opposite directions: (1) more rainout with uplift decreases $\delta^{18}O_p$ and (2) greater blocking of winter precipitation means that summer (high $\delta^{18}O_p$) accounts for a larger fraction of total annual precipitation, thereby increasing $\delta^{18}O_p$. These two effects are necessarily linked—lower $\delta^{18}O$ implies more windward rainout (effect 1), and more windward rainout implies less precipitation inland (effect 2). The clay mineral response in the lee (to the east) of uplift depends on which effect is greater. Results from a simple two end-member mixing model show that it is plausible for the seasonality effect to outpace the uplift effect, causing an increase in $\delta^{18}O_p$ with Cascades uplift that is consistent with the magnitude of the clay $\delta^{18}O$ increase (SI Text S4; Fig. S12).

The uplift of the Cascades is generally consistent with the relative changes in $\delta^{18}O$ across the OHT. Because the Cascades form a stronger winter rainshadow, we expect their uplift to have the largest effect on precipitation seasonality in the most winter-wet region. This is consistent with the largest clay $\delta^{18}O$ increase occurring in the west and the smallest in the east. Still, when analyzing the full dataset (rather than site-averaged $\delta^{18}O$) the increase in $\Delta\delta^{18}O_{clay-carb}$ in the west is dampened compared to the other domains due to an increase in carbonate $\delta^{18}O$ (statistically significant in the full dataset, but not site averaged $\delta^{18}O$). This increase in carbonate $\delta^{18}O$, if confirmed with more data, could be driven by a decrease in the prevalence of groundwater (lower-$\delta^{18}O$) carbonates that appear common near the OHT (SI Fig. 7), or a greater sensitivity of western domain carbonates to winter moisture due to a combination of a winter-dominant groundwater supply and low summer precipitation rates. The latter scenario is consistent with the apparent influence of winter-$\delta^{18}O$ in late Quaternary carbonates that form in the most winter-wet soils (SI Fig. S9). Additionally, the onset of soil carbonate formation just prior to the OHT and the apparent shift from groundwater to vadose zone carbonates across the OHT are consistent with the onset and strengthening of the dry Cascades rainshadow.

Despite its distance from the Cascades, the eastern domain is still hydrologically connected to the windward and leeward sides of the Cascades today (SI Fig. S13) and climate model simulations show that lower topography in this region would increase the winter precipitation fraction in the Great Plains in the past (Feng et al., 2013). Still, the eastern domain clay $\delta^{18}O$ increase appears delayed relative to the west (Fig. 2a). While more data will help determine the precise timing of these transitions, it is possible that greater summer moisture in the eastern domain prior to Cascades uplift dampened the increase in $\delta^{18}O$ from the seasonality effect, perhaps failing to reverse the opposing isotopic effect of uplift. In this case, the delayed increase in clay $\delta^{18}O$ may be attributable to the subsequent extension of the Basin and Range (*e.g.* (Dickinson, 2002; Loughney et al., 2021)) which would likely further restrict the supply of winter moisture by increasing orographic blocking of westerly and Arctic air-masses as well as the distance moisture must travel from the Pacific coast.

However, this hypothesis of Cascades uplift as the OHT driver remains speculative. The uplift history of the Cascades is debated (Takeuchi et al., 2010; Bershaw et al., 2019; McLean & Bershaw, 2021; Kohn & Fremd, 2007; Reiners et al., 2002; Methner, Fiebig, et al., 2016; Pesek et al., 2020), and while tectonic forcing can explain many aspects of our results, more isotope data (especially clay data) with robust age constraints are needed to rigorously test any links. Improved constraints on the spatial extent of the OHT would also help address the possibility that it was driven by Cascades uplift. Other open-habitat shifts occur globally in the Cenozoic, but generally asynchronously with one another and the timing presented herein (*e.g.* Strömberg et al. (2013); Karp et al. (2018); Andrae et al. (2018); Barbolini et al. (2020)). In the U.S., phytolith records outside of WCNA are sparse and limited to the last ∼17 million years. These data indicate grassy, open habitats in southern California by ∼17 Ma (Smiley et al., 2018; Loughney et al., 2020) and Kansas by at least 8 Ma (Strömberg & McInerney, 2011), but it is unclear if the onset of grassy conditions correlates with the WCNA signal. In general, phytolith preservation is poor south of WCNA. Nevertheless, whether tectonics is the underlying cause, the shift to drier winters provides new context to understand the drivers of grassland and open habitat expansion across the OHT.

4.4 Implications for OHT vegetation dynamics and biogeography

Our results support the hypothesis that the open habitat transition was a consequence of limited water availability (Harris et al., 2017; Wing, 1998; Webb & Opdyke, 1995; Wolfe, 1985) and, specifically, that drier winters decreased the annual supply of water by decreasing precipitation and spring snowmelt. However, changes in global temperature have also been proposed to trigger the OHT and while our results are unlikely to be driven by temperature (*e.g.* SI Fig. S4), we cannot rule out the possibility that temperature contributed to the OHT. A key line of evidence for temperature change is the expansion of pooid grasses, which tend to be adapted to cool or cold climates (Edwards & Smith, 2010; Schubert et al., 2019; Strömberg, 2005, 2011). However, many pooids also specialize in extreme aridity, and the lack of additional evidence for cooling suggests that drying can account for the pooid expansion (Edwards & Smith, 2010; Harris et al., 2017). Further, the survival of frost-intolerant palms across the OHT indicates that if cooling occurred, it must have been minor (Reichgelt et al., 2018; Strömberg, 2005, 2011). For now, any link between global temperature and the OHT remains ambiguous (Harris et al., 2017; Strömberg, 2011), but we suggest that neither warming nor cooling are required to explain grassland expansion across the OHT.

What do our results mean for the sensitivity of WCNA tree cover to climate? Much like WCNA tree cover today, forests spanning WCNA were likely reliant on winter precipitation before the OHT (Hu et al., 2010; Knowles et al., 2018; Berkelhammer et al., 2020). With the westerlies more easily traversing the Cascades (and Basin and Range) before the OHT, providing more winter moisture further inland, winter precipitation likely supported closed, wooded habitats as far east as the Great Plains. Still, it is not clear whether the expansion of open habitats occurred synchronously across WCNA, making it difficult to determine the precise conditions supporting greater forest coverage beyond wetter winters.

Even if the shift to drier winters occurred asynchronously, our finding that winter precipitation decreased in all domains may help explain why grass communities, unlike other aspects of WCNA floras, became more uniform from west to east after the OHT. Prior to the OHT bambusoid grasses were common in the understory of eastern domain forests but rare elsewhere, while after the OHT similar pooid-dominated, open-habitat communities expanded in at least the eastern and central domains (Strömberg, 2005; Miller et al., 2012). In contrast, woody taxa maintained their biogeographic affinities through and long after the OHT (Leopold & Denton, 1987; Strömberg, 2005, 2011). We suggest that greater water stress with winter drying across WCNA favored the expansion of open-habitat, primarily pooid-dominant grass communities during the OHT. Meanwhile, other aspects of plant communities, like woody taxa, likely persisted in places where conditions remained favorable.

A key implication of drier winters prompting grassland expansion is that grasses did not expand everywhere. Today, forests still prevail on mountain slopes that intercept westerly (winter) moisture and near perennial rivers that recharge groundwater (see Fig. 1e) (Schimel et al., 2002). A shift to drier winters probably decreased precipitation in the intermontane valleys that cover much of the WCNA or on east-facing slopes that do not intercept westerly moisture. Orographic precipitation and perennial rivers are reliable moisture sources in places that do intercept the westerlies, thus dampening the decrease in winter precipitation and supporting tree cover in these regions. In addition to orographic precipitation, colder temperatures at higher elevation help preserve snowpack and limit evaporation in the warm, growing season, further maintaining the water supply (Clow, 2010; Hu et al., 2010). We hypothesize that the open habitat transition was predominantly a low-relief (and east-facing slope) phenomenon and vegetation fed by orographic precipitation or groundwater from perennial rivers was not as severely impacted.

The aridification associated with the OHT reorganized WCNA floral and faunal communities and may have increased mammal diversity. Phytolith indicators of forests, closed habitat grasses, and moisture-dependent gingers and palms are all present after the OHT, just in much lower abundances (Strömberg, 2005). The survival of these floras while open, grassy habitats expanded likely dampened the loss of mammals adapted to forests while promoting the niche-filling diversification of mammals adapted to new, open habitats (Samuels & Hopkins, 2017). The number of mesodont and hypsodont taxa (adapted to eating silica-rich vegetation in dusty environments like grasslands) increased in both small and large mammalian herbivores near the start and end of the OHT, respectively (Janis et al., 2000; Jardine et al., 2012; Samuels & Hopkins, 2017). This increase in taxonomic richness, however, appears short-lived—each niche-filling pulse is followed by a subsequent decline in taxonomic richness driven by the loss of taxa adapted to feeding on trees and shrubs, less likely to be covered in dust (Janis et al., 2000; Samuels & Hopkins, 2017; Jardine et al., 2012).

Overall, we suggest that winter drying triggered the expansion of open, grassy habitats by decreasing winter precipitation and spring and summer snowmelt, and increasing forest water stress. Forests relied on winter precipitation before the OHT, as they do today, and drier winters would have inhibited forest survival, allowing open habitat grasslands to expand. Other factors like fire frequency and intensity may have also promoted grassland expansion by reducing summer soil moisture, but charcoal data and organic biomarker data of fire are sparse and more data are needed to test this hypothesis. Drier winters across the open habitat transition mark a shift to more mosaic landscapes with the expansion of open, grassy ecosystems representing an important step from the closed-forest vegetation of the Paleogene to the grasslands, scrublands, and deserts that span WCNA today.

5 Concluding remarks

Our results refute the hypothesis that drier summers caused grassland expansion across the OHT (Retallack, 2004b) and instead implicate drier winters due to a decrease in the contribution of westerly precipitation. The cause of winter drying, however, remains unknown. Topography sets the step-wise spatial gradient of WCNA precipitation seasonality today and we tentatively suggest that tectonic change, namely the uplift of the Cascades, caused drier winters across the OHT. Still, more data and rigorous model analysis are needed to test if this is compatible with the isotope record.

The expansion of open-habitat communities with drier winters across the OHT demonstrates that the modern, positive relationship between winter precipitation and western U.S. biomass, productivity, and tree cover (Hu et al., 2010; Knowles et al., 2017, 2018; Berkelhammer et al., 2020) has existed since the Eocene. Our findings suggests that the link between winter precipitation and vegetation is robust over time and across timescales. Drier winters can decrease WCNA biomass on short ($< 10^2$yr) and long ($> 10^6$yr) timescales despite differences in the time available for plant communities to adapt. As winter moisture declines with ongoing warming, our study emphasizes the fundamental challenges that WCNA forests face when winter water is limited.

Acknowledgments

We acknowledge H.T. Mix and D.Y. Moragne for isotope compilation assistance and T.M. Schwartz and K. Methner for field assistance. We also thank J. Payne for advice on the statistical handling of the data. Elevation data are sourced from Terrain Tiles hosted on Amazon Web Services. Terrain Tiles data combines Global ETOPO1 and 3DEP datasets. Global ETOPO1 terrain data is courtesy of the U.S. National Oceanic and Atmospheric Administration. United States 3DEP (formerly NED) and global GMTED2010 and SRTM terrain data are courtesy of the U.S. Geological Survey. Research at John Day Fossil Beds National Monument was conducted under Study Number JODA-00033 with Permit Numbers JODA-2017-SCI-001 and JODA-2018-SCI-002, issued by John Day Fossil Beds and the United States Department of the Interior National Park Service. Isotope and phytolith data in this manuscript can be found in the supporting material. Funding for this research is provided by NSF grants EAR-1253713 to CAES and EAR-1450357 to CPC.

References

Allen, S. T., Kirchner, J. W., Braun, S., Siegwolf, R. T. W., & Goldsmith, G. R. (2019, March). Seasonal origins of soil water used by trees. *Hydrology and Earth System Sciences*, *23*(2), 1199–1210. doi: 10.5194/hess-23-1199-2019

Amundson, R., Chadwick, O., Kendall, C., & Wang, Y. (1996). Isotopic evidence for shifts in atmospheric circulation patterns during the late Quaternary in mid–North America. *Geology*, *24*(1969), 23–26. doi: 10.1130/0091-7613

Andrae, J. W., Mcinerney, F. A., Polissar, P. J., Sniderman, J. M. K., & Howard, S. (2018). Initial Expansion of C 4 Vegetation in Australia During the Late Pliocene. *Geophysical Research Letters*(May), 1–10. doi: 10.1029/2018GL077833

Axelrod, D. I. (1998). The Oligocene Haynes Creek Flora of Eastern Idaho. *University of California Publications on Geological Sciences*, *143*, 99.

Badgley, C., & Finarelli, J. A. (2013). Diversity dynamics of mammals in relation to tectonic and climatic history: Comparison of three Neogene records from North America. *Paleobiology*, *39*(3), 373–399. doi: 10.1666/12024

Badgley, C., Smiley, T. M., Terry, R., Davis, E. B., DeSantis, L. R., Fox, D. L., ... Yanites, B. J. (2017, March). Biodiversity and Topographic Complexity: Modern and Geohistorical Perspectives. *Trends in Ecology & Evolution*, *32*(3), 211–226. doi: 10.1016/j.tree.2016.12.010

Barbolini, N., Woutersen, A., Dupont-Nivet, G., Silvestro, D., Tardif, D., Coster, P. M. C., ... Hoorn, C. (2020, October). Cenozoic evolution of the steppe-desert biome in Central Asia. *Science Advances*, *6*(41), eabb8227. doi: 10.1126/sciadv.abb8227

Barboni, D., Bremond, L., & Bonnefille, R. (2007, April). Comparative study of modern phytolith assemblages from inter-tropical Africa. *Palaeogeography, Palaeoclimatology, Palaeoecology*, *246*(2-4), 454–470. doi: 10.1016/j.palaeo.2006.10.012

Barnes, C. J., & Allison, G. B. (1983). The Distribution of Deuterium and 180 in Dry Soils 1: Theory. *Journal of Hydrology*, *60*, 141–156.

Berkelhammer, M., Stefanescu, I. C., Joiner, J., & Anderson, L. (2017, April). High sensitivity of gross primary production in the Rocky Mountains to summer rain. *Geophysical Research Letters*, *44*(8), 3643–3652. doi: 10.1002/2016GL072495

Berkelhammer, M., Still, C. J., Ritter, F., Winnick, M., Anderson, L., Carroll, R., ... Williams, K. H. (2020, February). Persistence and Plasticity in Conifer

Water-Use Strategies. *Journal of Geophysical Research: Biogeosciences*, *125*(2). doi: 10.1029/2018JG004845

Bershaw, J., Cassel, E. J., Carlson, T. B., Streig, A. R., & Streck, M. J. (2019, September). Volcanic glass as a proxy for Cenozoic elevation and climate in the Cascade Mountains, Oregon, USA. *Journal of Volcanology and Geothermal Research*, *381*, 157–167. doi: 10.1016/j.jvolgeores.2019.05.021

Bestland, E. A., Hammond, P. E., Blackwell, D. L. S., Kays, M. A., Retallack, G. J., & Stimac, J. (2002). Geologic Framework of the Clarno Unit, John Day Fossil Beds National Monument, Central Oregon. *Oregon Department of Geology and Mineral Industries Open-File Report*, 1–39.

Bestland, E. A., Retallack, G. J., & Swisher III, C. C. (1997). Stepwise Climate Change Recorded in Eocene-Oligocene Paleosol Sequences From Central Oregon. *The Journal of Geology*, *105*(2), 153–172. doi: 10.1086/515906

Bird, M. I., Longstaffe, F. J., Fyfe, W. S., Kronberg, B. I., & Kishida, A. (1993). An Oxygen-Isotope Study of Weathering in the Eastern Amazon Basin, Brazil. *Climate Change in Continental Isotopic Records*, 295–307. doi: 10.1029/GM078p0295

Breecker, D., Sharp, Z., & McFadden, L. (2009, March). Seasonal bias in the formation and stable isotopic composition of pedogenic carbonate in modern soils from central New Mexico, USA. *Geological Society of America Bulletin*, *121*(3-4), 630–640. doi: 10.1130/B26413.1

Caves, J. K., Moragne, D. Y., Ibarra, D. E., Bayshashov, B. U., Gao, Y., Jones, M. M., ... Chamberlain, C. P. (2016). The Neogene de-greening of Central Asia. *Geology*, *44*(11), in press. doi: 10.1130/G38267.1

Chamberlain, C. P., Mix, H. T., Mulch, A., Hren, M. T., Kent-Corson, M. L., Davis, S. J., ... Graham, S. A. (2012). The cenozoic climatic and topographic evolution of the western north American Cordillera. *American Journal of Science*, *312*(2), 213–262. doi: 10.2475/02.2012.05

Chamberlain, C. P., Winnick, M. J., Mix, H. T., Chamberlain, S. D., & Maher, K. (2014). The impact of neogene grassland expansion and aridification on the isotopic composition of continental precipitation. *Global Biogeochemical Cycles*, *28*(9), 992–1004. doi: 10.1002/2014GB004822

Chen, S. T., Smith, S. Y., Sheldon, N. D., & Strömberg, C. A. (2015, November). Regional-scale variability in the spread of grasslands in the late Miocene. *Palaeogeography, Palaeoclimatology, Palaeoecology*, *437*, 42–52. doi: 10.1016/j.palaeo.2015.07.020

Clow, D. W. (2010, May). Changes in the Timing of Snowmelt and Streamflow in Colorado: A Response to Recent Warming. *Journal of Climate*, *23*(9), 2293–2306. doi: 10.1175/2009JCLI2951.1

Cotton, J. M., Sheldon, N. D., & Strömberg, C. A. (2012, June). High-resolution isotopic record of C4 photosynthesis in a Miocene grassland. *Palaeogeography, Palaeoclimatology, Palaeoecology*, *337–338*, 88–98. doi: 10.1016/j.palaeo.2012.03.035

Crifò, C., & Strömberg, C. A. (2020, January). Small-scale spatial resolution of the soil phytolith record in a rainforest and a dry forest in Costa Rica: Applications to the deep-time fossil phytolith record. *Palaeogeography, Palaeoclimatology, Palaeoecology*, *537*, 109107. doi: 10.1016/j.palaeo.2019.03.008

Crifò, C., & Strömberg, C. A. (2021, January). Spatial patterns of soil phytoliths in a wet vs. dry neotropical forest: Implications for paleoecology. *Palaeogeography, Palaeoclimatology, Palaeoecology*, *562*, 110100. doi: 10.1016/j.palaeo.2020.110100

Dansgaard, W. (1964). Stable isotopes in precipitation. *Tellus*, *16*(4), 436–468. doi: 10.3402/tellusa.v16i4.8993

Database, W. (2019). Retrieved from http://waterisotopes.org. Accessed 7/13/2019. Query: NLat=51, SLat=38, ELon=-90, WLon=-130, Type=Precipitation.

Dickinson, W. R. (2002, January). The Basin and Range Province as a Composite Extensional Domain. *International Geology Review*, *44*(1), 1–38. doi: 10.2747/0020-6814.44.1.1

Dillhoff, R. M., Dillhoff, T. A., Jijina, A. P., & Strömberg, C. A. E. (2014). The Vasa Park Flora, King county, Washington, U.S.A: A Window into the Late Miocene of the Pacific Northwest. In *Paleobotany and biogeography, a Festschrift for Alan Graham in His 80th Year* (pp. 64–97). St. Louis, Missouri: Missouri Botanical Garden Press.

Dunlap, D. (1982). *Tertiary Geology of the Muddy Creek Basin, Beaverhead County, Montana* (M.S. Thesis). University of Montana, Missoula, Montana.

Edwards, E. J., & Smith, S. A. (2010, February). Phylogenetic analyses reveal the shady history of C4 grasses. *Proceedings of the National Academy of Sciences*, *107*(6), 2532–2537. doi: 10.1073/pnas.0909672107

Emry, R. J. (1973). Stratigraphy and Preliminary Biostratigraphy of the Flagstaff Rim Area, Natrona County, Wyoming. *Smithsonian Contributions to Paleobiology*(18), 1–43. doi: 10.5479/si.00810266.18.1

Emry, R. J. (1992, December). Mammalian Range Zones in the Chadronian White River Formation at Flagstaff Rim, Wyoming. In D. R. Prothero & W. A. Berggren (Eds.), *Eocene-Oligocene Climatic and Biotic Evolution* (pp. 106–115). Princeton University Press. doi: 10.1515/9781400862924.106

Evernden, J. F., Savage, D. E., Curtis, G. H., & James, G. T. (1964, February). Potassium-argon dates and the Cenozoic mammalian chronology of North America. *American Journal of Science*, *262*(2), 145–198. doi: 10.2475/ajs.262.2.145

Fan, M., Ayyash, S. A., Tripati, A., Passey, B. H., & Griffith, E. M. (2018, July). Terrestrial cooling and changes in hydroclimate in the continental interior of the United States across the Eocene-Oligocene boundary. *GSA Bulletin*, *130*(7-8), 1073–1084. doi: 10.1130/B31732.1

Fan, M., Heller, P., Allen, S. D., & Hough, B. G. (2014, June). Middle Cenozoic uplift and concomitant drying in the central Rocky Mountains and adjacent Great Plains. *Geology*, *42*(6), 547–550. doi: 10.1130/G35444.1

Feng, R., Poulsen, C. J., Werner, M., Chamberlain, C. P., Mix, H. T., & Mulch, A. (2013, September). Early Cenozoic evolution of topography, climate, and stable isotopes in precipitation in the North American Cordillera. *American Journal of Science*, *313*(7), 613–648. doi: 10.2475/07.2013.01

Fox, D. L., & Koch, P. L. (2003). Tertiary history of C4 biomass in the Great Plains, USA. *Geology*, *31*(9), 809. doi: 10.1130/G19580.1

Fox, D. L., & Koch, P. L. (2004). Carbon and oxygen isotopic variability in Neogene paleosol carbonates: Constraints on the evolution of the C4-grasslands of the Great Plains, USA. *Palaeogeography, Palaeoclimatology, Palaeoecology*, *207*(3-4), 305–329. doi: 10.1016/S0031-0182(04)00045-8

Gallagher, T. M., Hren, M., & Sheldon, N. D. (2019, September). The effect of soil temperature seasonality on climate reconstructions from paleosols. *American Journal of Science*, *319*(7), 549–581. doi: 10.2475/07.2019.02

Gallagher, T. M., & Sheldon, N. D. (2016, October). Combining soil water balance and clumped isotopes to understand the nature and timing of pedogenic carbonate formation. *Chemical Geology*, *435*, 79–91. doi: 10.1016/j.chemgeo.2016.04.023

Gao, Y., Ibarra, D. E., Caves Rugenstein, J. K., Chen, J., Kukla, T., Methner, K., ... Wang, C. (2021, May). Terrestrial climate in mid-latitude East Asia from the latest Cretaceous to the earliest Paleogene: A multiproxy record from the Songliao Basin in northeastern China. *Earth-Science Reviews*, *216*, 103572. doi: 10.1016/j.earscirev.2021.103572

Geospatial Information Authority of Japan, Chiba University, & Collaborating Organizations. (2016). Vegetation (Percent Tree Cover) - Global Version -

Version 1. *Globalmaps*.

Grass Phylogeny Working Group II. (2012, January). New grass phylogeny resolves deep evolutionary relationships and discovers C4 origins. *New Phytologist*, *193*(2), 304–312. doi: 10.1111/j.1469-8137.2011.03972.x

Harris, E. B., Strömberg, C. A., Sheldon, N. D., Smith, S. Y., & Vilhena, D. A. (2017, November). Vegetation response during the lead-up to the middle Miocene warming event in the Northern Rocky Mountains, USA. *Palaeogeography, Palaeoclimatology, Palaeoecology*, *485*, 401–415. doi: 10.1016/j.palaeo.2017.06.029

Harrison, S. (1985). *Sedimentology of Tertiary Sedimentary Rocks near Salmon, Idaho* (Unpublished doctoral dissertation). University of Montana, Missoula, Montana.

Hillel, D. (1982). *Introduction to Soil Physics.* New York, NY: Academic Press, Inc.

Hollister, J., Shah, T., Robitaille, A. L., Beck, M. W., & Johnson, M. (2021). *Elevatr: Access Elevation Data from Various APIs.*

Horton, T., Sjostrom, D., Abruzzese, M., Poage, M., Waldbauer, J., Hren, M., ... Chamberlain, C. (2004). Spatial and temporal variation of Cenozoic surface elevation in the Great Basin and Sierra Nevada. *American Journal of Science*, *304*(650), 862–888.

Hu, J., Moore, D. J. P., Burns, S. P., & Monson, R. K. (2010, February). Longer growing seasons lead to less carbon sequestration by a subalpine forest. *Global Change Biology*, *16*(2), 771–783. doi: 10.1111/j.1365-2486.2009.01967.x

Hunt, R. M. (1990). Taphonomy and sedimentology of Arikaree (lower Miocene) fluvial, eolian, and lacustrine paleoenvironments, Nebraska and Wyoming; A paleobiota entombed in fine-grained volcaniclastic rocks. In *Geological Society of America Special Papers* (Vol. 244, pp. 69–112). Geological Society of America. doi: 10.1130/SPE244-p69

Huth, T. E., Cerling, T. E., Marchetti, D. W., Bowling, D. R., Ellwein, A. L., & Passey, B. H. (2019, March). Seasonal Bias in Soil Carbonate Formation and Its Implications for Interpreting High-Resolution Paleoarchives: Evidence From Southern Utah. *Journal of Geophysical Research: Biogeosciences*, *124*(3), 616–632. doi: 10.1029/2018JG004496

Hyland, E. G., Sheldon, N. D., Smith, S. Y., & Strömberg, C. A. (2019, January). Late Miocene rise and fall of C4 grasses in the western United States linked to aridification and uplift. *GSA Bulletin*, *131*(1-2), 224–234. doi: 10.1130/B32009.1

Iriarte, J., & Paz, E. A. (2009, January). Phytolith analysis of selected native plants and modern soils from southeastern Uruguay and its implications for paleoenvironmental and archeological reconstruction. *Quaternary International*, *193*(1-2), 99–123. doi: 10.1016/j.quaint.2007.10.008

Janecke, S., & Blankenau, J. C. (2003). Extensional folds associated with Paleogene detachment faults in SE part of the Salmon Basin. *Northwest Geology*, *32*, 51.

Janecke, S., McIntosh, W., & Good, S. (1999, June). Testing models of rift basins: Structure and stratigraphy of an Eocene-Oligocene supradetachment basin, Muddy Creek half graben, south-west Montana: Testing supradetachment basin models. *Basin Research*, *11*(2), 143–165. doi: 10.1046/j.1365-2117.1999.00092.x

Janis, C. M., Damuth, J., & Theodor, J. M. (2000, July). Miocene ungulates and terrestrial primary productivity: Where have all the browsers gone? *Proceedings of the National Academy of Sciences*, *97*(14), 7899–7904. doi: 10.1073/pnas.97.14.7899

Jardine, P. E., Janis, C. M., Sahney, S., & Benton, M. J. (2012, December). Grit not grass: Concordant patterns of early origin of hypsodonty in Great Plains ungulates and Glires. *Palaeogeography, Palaeoclimatology, Palaeoecology*, *365–366*, 1–10. doi: 10.1016/j.palaeo.2012.09.001

Jasechko, S., Birks, S. J., Gleeson, T., Wada, Y., Fawcett, P. J., Sharp, Z. D., ... Welker, J. M. (2014, November). The pronounced seasonality of global groundwater recharge. *Water Resources Research*, *50*(11), 8845–8867. doi: 10.1002/2014WR015809

Karp, A. T., Behrensmeyer, A. K., & Freeman, K. H. (2018, November). Grassland fire ecology has roots in the late Miocene. *Proceedings of the National Academy of Sciences*, *115*(48), 12130–12135. doi: 10.1073/pnas.1809758115

Kelson, J. R., Huntington, K. W., Breecker, D. O., Burgener, L. K., Gallagher, T. M., Hoke, G. D., & Petersen, S. V. (2020, April). A proxy for all seasons? A synthesis of clumped isotope data from Holocene soil carbonates. *Quaternary Science Reviews*, *234*, 106259. doi: 10.1016/j.quascirev.2020.106259

Kendall, C., & Coplen, T. B. (2001). Distribution of oxygen-18 and deuterium in river waters across the United States. *Hydrological Processes*, *15*(7), 1363–1393. doi: 10.1002/hyp.217

Kent-Corson, M. L., Barnosky, A. D., Mulch, A., Carrasco, M. A., & Chamberlain, C. P. (2013). Possible regional tectonic controls on mammalian evolution in western North America. *Palaeogeography, Palaeoclimatology, Palaeoecology*, *387*, 17–26. doi: 10.1016/j.palaeo.2013.07.014

Kent-Corson, M. L., Mulch, A., Graham, S. A., Carroll, A. R., Ritts, B. D., & Chamberlain, C. P. (2010). Diachronous isotopic and sedimentary responses to topographic change as indicators of mid-Eocene hydrologic reorganization in the western United States. *Basin Research*, *22*(6), 829–845. doi: 10.1111/j.1365-2117.2009.00456.x

Kent-Corson, M. L., Sherman, L. S., Mulch, A., & Chamberlain, C. P. (2006). Cenozoic topographic and climatic response to changing tectonic boundary conditions in Western North America. *Earth and Planetary Science Letters*, *252*(3-4), 453–466. doi: 10.1016/j.epsl.2006.09.049

Kim, S.-T., & O'Neil, J. R. (1997). Equilibrium and nonequilibrium oxygen isotope effects in synthetic carbonates. *Geochimica et Cosmochimica Acta*, *61*(16), 3461–3475. doi: 10.1016/S0016-7037(97)00169-5

Knowles, J. F., Lestak, L. R., & Molotch, N. P. (2017, June). On the use of a snow aridity index to predict remotely sensed forest productivity in the presence of bark beetle disturbance. *Water Resources Research*, *53*(6), 4891–4906. doi: 10.1002/2016WR019887

Knowles, J. F., Molotch, N. P., Trujillo, E., & Litvak, M. E. (2018, April). Snowmelt-Driven Trade-Offs Between Early and Late Season Productivity Negatively Impact Forest Carbon Uptake During Drought. *Geophysical Research Letters*, *45*(7), 3087–3096. doi: 10.1002/2017GL076504

Kohn, M. J., & Fremd, T. J. (2007). Tectonic controls on isotope compositions and species diversification, John Day Basin, central Oregon. *PaleoBios*, *27*(2), 14.

Kukla, T., Ibarra, D., Caves Rugenstein, J. K., Gooley, J. T., Mullins, C., Kramer, S., ... Chamberlain, C. P. (2021). High-Resolution Stable Isotope Paleotopography of the John Day Region, Oregon, United States. *Frontiers in Earth Science*, *9*, 9.

Kukla, T., Winnick, M. J., Maher, K., Ibarra, D. E., & Chamberlain, C. P. (2019, January). The Sensitivity of Terrestrial δ [18] O Gradients to Hydroclimate Evolution. *Journal of Geophysical Research: Atmospheres*, *124*, 563–582. doi: 10.1029/2018JD029571

Lawrence, J. R., & Taylor, H. P. (1971). Deuteritun and oxygen-18 correlation: Clay minerals and hydroxides in Quaternarysoils compared to meteoric waters. *Geochimica et Cosmochimica Acta*, *35*, 993–1003.

Lee, J.-E., & Fung, I. (2008). "Amount effect" of water isotopes and quantitative analysis of post-condensation processes. *Hydrological Processes*, *2274*(November 2008), 2267–2274. doi: 10.1002/hyp

Leopold, E. B., & Denton, M. F. (1987). Comparative Age of Grassland and Steppe

East and West of the Northern Rocky Mountain. *Annals of the Missouri Botanical Garden*, *74*(4), 841. doi: 10.2307/2399452

Licht, A., Dupont-Nivet, G., Meijer, N., Caves Rugenstein, J., Schauer, A., Fiebig, J., ... Guo, Z. (2020, December). Decline of soil respiration in northeastern Tibet through the transition into the Oligocene icehouse. *Palaeogeography, Palaeoclimatology, Palaeoecology*, *560*, 110016. doi: 10.1016/j.palaeo.2020.110016

Liu, B., Phillips, F. M., & Campbell, A. R. (1996, September). Stable carbon and oxygen isotopes of pedogenic carbonates, Ajo Mountains, southern Arizona: Implications for paleoenvironmental change. *Palaeogeography, Palaeoclimatology, Palaeoecology*, *124*(3-4), 233–246. doi: 10.1016/0031-0182(95)00093-3

Liu, Z., Bowen, G. J., & Welker, J. M. (2010). Atmospheric circulation is reflected in precipitation isotope gradients over the conterminous United States. *Journal of Geophysical Research Atmospheres*, *115*(22), 1–14. doi: 10.1029/2010JD014175

Lora, J. M., & Ibarra, D. E. (2019, December). The North American hydrologic cycle through the last deglaciation. *Quaternary Science Reviews*, *226*, 105991. doi: 10.1016/j.quascirev.2019.105991

Loughney, K. M., Badgley, C., Bahadori, A., Holt, W. E., & Rasbury, E. T. (2021, November). Tectonic influence on Cenozoic mammal richness and sedimentation history of the Basin and Range, western North America. *Science Advances*, *7*(45), eabh4470. doi: 10.1126/sciadv.abh4470

Loughney, K. M., Hren, M. T., Smith, S. Y., & Pappas, J. L. (2020, January). Vegetation and habitat change in southern California through the Middle Miocene Climatic Optimum: Paleoenvironmental records from the Barstow Formation, Mojave Desert, USA. *GSA Bulletin*, *132*(1-2), 113–129. doi: 10.1130/B35061.1

Maher, K., Steefel, C. I., White, A. F., & Stonestrom, D. A. (2009, May). The role of reaction affinity and secondary minerals in regulating chemical weathering rates at the Santa Cruz Soil Chronosequence, California. *Geochimica et Cosmochimica Acta*, *73*(10), 2804–2831. doi: 10.1016/j.gca.2009.01.030

McInerney, F. A., Strömberg, C. A. E., & James, W. W. (2011). The Neogene transition from C3 to C4 grasslands in North America: Stable carbon isotope ratios of fossil phytoliths America. *Paleobiology*, *37*(1), 23–49. doi: 10.1666/09068.1

McLean, A., & Bershaw, J. (2021, March). Molecules to Mountains: A Multi-Proxy Investigation Into Ancient Climate and Topography of the Pacific Northwest, USA. *Frontiers in Earth Science*, *9*, 624961. doi: 10.3389/feart.2021.624961

Methner, K. (2015). *Recovering Eocene paleotopography and paleoclimate of the North American Cordillera through integrated stable isotope and clumped isotope analyses* (Unpublished doctoral dissertation). Goethe University, Frankfurt, Germany.

Methner, K., Fiebig, J., Wacker, U., Umhoefer, P., Chamberlain, C. P., & Mulch, A. (2016). Eocene-Oligocene proto-Cascades topography revealed by clumped (Δ47) and oxygen isotope (δ18O) geochemistry (Chumstick Basin, WA, USA). *Tectonics*, *35*(3), 546–564. doi: 10.1002/2015TC003984

Methner, K., Mulch, A., Fiebig, J., Wacker, U., Gerdes, A., Graham, S. A., & Chamberlain, C. P. (2016). Rapid Middle Eocene temperature change in western North America. *Earth and Planetary Science Letters*, *450*, 132–139. doi: 10.1016/j.epsl.2016.05.053

Meyer, N. A., Breecker, D. O., Young, M. H., & Litvak, M. E. (2014, May). Simulating the Effect of Vegetation in Formation of Pedogenic Carbonate. *Soil Science Society of America Journal*, *78*(3), 914–924. doi: 10.2136/sssaj2013.08.0326

M'Gonigle, J., & Dalrymple, G. (1993). 40Ar/39Ar ages of Challis volcanic rocks and the initiation of Tertiary sedimentary basins in southwestern Montana.

The Mountain Geologist, *30*, 112–118.
Miller, L. A., Smith, S. Y., Sheldon, N. D., & Strömberg, C. A. E. (2012, September). Eocene vegetation and ecosystem fluctuations inferred from a high-resolution phytolith record. *Geological Society of America Bulletin*, *124*(9-10), 1577–1589. doi: 10.1130/B30548.1
Mix, H. T., & Chamberlain, C. P. (2014). Stable isotope records of hydrologic change and paleotemperature from smectite in Cenozoic western North America. *Geochimica et Cosmochimica Acta*, *141*, 532–546. doi: 10.1016/j.gca.2014.07.008
Mix, H. T., Ibarra, D. E., Mulch, A., Graham, S. A., & Page Chamberlain, C. (2016). A hot and high Eocene Sierra Nevada. *Bulletin of the Geological Society of America*, *128*(3-4), 531–542. doi: 10.1130/B31294.1
Mix, H. T., Winnick, M. J., Mulch, A., & Page Chamberlain, C. (2013). Grassland expansion as an instrument of hydrologic change in Neogene western North America. *Earth and Planetary Science Letters*, *377–378*, 73–83. doi: 10.1016/j.epsl.2013.07.032
Morrill, C., & Koch, P. L. (2002). Elevation or alteration? Evaluation of isotopic constraints on paleoaltitudes surrounding the Eocene Green River Basin. *Geology*, *30*(4), 151–154.
Mulch, A., Chamberlain, C. P., Cosca, M. A., Teyssier, C., Methner, K., Hren, M. T., & Graham, S. A. (2015). Rapid change in high-elevation precipitation patterns of Western North America during the Middle Eocene Climatic Optimum (MECO). *American Journal of Science*, *315*(4), 317–336. doi: 10.2475/04.2015.02
Mullin, M. R. D. (2010). *Stable isotope record of soil carbonates from the Eocene-Oligocene transition, Badlands National Park, South Dakota, USA* (MS). Ball State University, Muncie, IN.
Norris, R. D., Jones, L. S., Corfield, R. M., & Cartlidge, J. E. (1996). Skiing in the Eocene Uinta Mountains? Isotopic evidence in the Green River Formation for snow melt and large mountains. *Geology*, *24*(5), 403–406.
Novello, A., Barboni, D., Berti-Equille, L., Mazur, J.-C., Poilecot, P., & Vignaud, P. (2012, June). Phytolith signal of aquatic plants and soils in Chad, Central Africa. *Review of Palaeobotany and Palynology*, *178*, 43–58. doi: 10.1016/j.revpalbo.2012.03.010
Oerter, E. J., Sharp, W. D., Oster, J. L., Ebeling, A., Valley, J. W., Kozdon, R., … Amundson, R. (2016, January). Pedothem carbonates reveal anomalous North American atmospheric circulation 70,000–55,000 years ago. *Proceedings of the National Academy of Sciences*, *113*(4), 919–924. doi: 10.1073/pnas.1515478113
Oster, J. L., Ibarra, D. E., Winnick, M. J., & Maher, K. (2015). Steering of westerly storms over western North America at the Last Glacial Maximum. *Nature Geoscience*, *8*(February), 201–205. doi: 10.1038/NGEO2365
Palandri, J. L., & Kharaka, Y. K. (2004). *A Compilation of Rate Parameters of Water-Mineral Interaction Kinetics for Application to Geochemical Modeling* (Open-File Report No. 2004-1068). Washington, D. C.: U.S. Department of Interior, U.S. Geological Survey.
Pesek, M. E., Perez, N. D., Meigs, A., Rowden, C. C., & Giles, S. M. (2020, September). Exhumation Timing in the Oregon Cascade Range Decoupled From Deformation, Magmatic, and Climate Patterns. *Tectonics*, *39*(9). doi: 10.1029/2020TC006078
Peters, N. A., Huntington, K. W., & Hoke, G. D. (2013, January). Hot or not? Impact of seasonally variable soil carbonate formation on paleotemperature and O-isotope records from clumped isotope thermometry. *Earth and Planetary Science Letters*, *361*, 208–218. doi: 10.1016/j.epsl.2012.10.024
Poage, M. A., & Chamberlain, C. P. (2002). Stable isotopic evidence for a Pre-

Middle Miocene rain shadow in the western Basin and Range: Implications for the paleotopography of the Sierra Nevada. *Tectonics*, *21*(4), 1034. doi: 10.1029/2001TC001303

Poppe, L. J., Paskevich, V. F., Hathaway, J., & Blackwood, D. (2001). *A laboratory manual for X-ray powder diffraction* (- ed.; Report No. 2001-41). doi: 10.3133/ofr0141

PRISM, C. G. (2012). PRISM Climate Group, Oregon State University, http://prism.oregonstate.edu, created 20 Jul 2012. Accessed 3 Sep. 2020.

Quade, J., & Cerling, T. E. (1995). Expansion of C4 grasses in the Late Miocene of Northern Pakistan: Evidence from stable isotopes in paleosols. *Palaeogeography, Palaeoclimatology, Palaeoecology*, *115*(1-4), 91–116. doi: 10.1016/0031-0182(94)00108-K

Quade, J., Cerling, T. E., & Bowman, J. R. (1989, April). Systematic variations in the carbon and oxygen isotopic composition of pedogenic carbonate along elevation transects in the southern Great Basin, United States. *Geological Society of America Bulletin*, *101*(4), 464–475. doi: 10.1130/0016-7606(1989)101<0464:SVITCA>2.3.CO;2

Reichgelt, T., West, C. K., & Greenwood, D. R. (2018, December). The relation between global palm distribution and climate. *Scientific Reports*, *8*(1), 4721. doi: 10.1038/s41598-018-23147-2

Reiners, P. W., Ehlers, T. A., Garver, J. I., Mitchell, S. G., Montgomery, D. R., Vance, J. A., & Nicolescu, S. (2002). Late Miocene exhumation and uplift of the Washington Cascade Range. *Geology*, *30*(9), 767. doi: 10.1130/0091-7613(2002)030<0767:LMEAUO>2.0.CO;2

Retallack, G. J. (2001). Cenozoic Expansion of Grasslands and Climatic Cooling. *Journal of Geology*, *109*, 407–426.

Retallack, G. J. (2004a, November). Late Miocene climate and life on land in Oregon within a context of Neogene global change. *Palaeogeography, Palaeoclimatology, Palaeoecology*, *214*(1-2), 97–123. doi: 10.1016/S0031-0182(04)00394-3

Retallack, G. J. (2004b, May). Late Oligocene bunch grassland and early Miocene sod grassland paleosols from central Oregon, USA. *Palaeogeography, Palaeoclimatology, Palaeoecology*, *207*(3-4), 203–237. doi: 10.1016/j.palaeo.2003.09.027

Retallack, G. J. (2013, May). Global Cooling by Grassland Soils of the Geological Past and Near Future. *Annual Review of Earth and Planetary Sciences*, *41*(1), 69–86. doi: 10.1146/annurev-earth-050212-124001

Retallack, G. J., Orr, W. N., Prothero, D. R., Duncan, R. A., Kester, P. R., & Ambers, C. P. (2004). Eocene-Oligocene extinction and paleoclimatic change near Eugene, Oregon. *Geological Society of America Bulletin*, *116*(7), 817. doi: 10.1130/B25281.1

Retallack, G. J., Wynn, J. G., & Fremd, T. J. (2004). Glacial-interglacial-scale paleoclimatic change without large ice sheets in the Oligocene of central Oregon. *Geology*, *32*(4), 297–300. doi: 10.1130/G20247.1

R Team, R. (2021). *R: A language and environment for statistical computing.* R Foundation for Statistical Computing. Vienna, Austria.

Rugenstein, J. K., & Chamberlain, C. P. (2018, September). The evolution of hydroclimate in Asia over the Cenozoic: A stable-isotope perspective. *Earth-Science Reviews*. doi: 10.1016/j.earscirev.2018.09.003

Rutz, J. J., Steenburgh, W. J., & Ralph, F. M. (2014, February). Climatological Characteristics of Atmospheric Rivers and Their Inland Penetration over the Western United States. *Monthly Weather Review*, *142*(2), 905–921. doi: 10.1175/MWR-D-13-00168.1

Salati, E., Dall'Olio, A., Matsui, E., & Gat, J. R. (1979). Recycling of water in the Amazon Basin: An isotopic study. *Water Resources Research*, *15*(5), 1250–1258. doi: 10.1029/WR015i005p01250

Samuels, J. X., & Hopkins, S. S. (2017, February). The impacts of Cenozoic climate and habitat changes on small mammal diversity of North America. *Global and Planetary Change*, *149*, 36–52. doi: 10.1016/j.gloplacha.2016.12.014

Savin, S. M., & Epstein, S. (1970, January). The oxygen and hydrogen isotope geochemistry of clay minerals. *Geochimica et Cosmochimica Acta*, *34*(1), 25–42. doi: 10.1016/0016-7037(70)90149-3

Schimel, D., Kittel, T. G. F., Running, S., Monson, R., Turnipseed, A., & Anderson, D. (2002). Carbon sequestration studied in western U.S. mountains. *Eos, Transactions American Geophysical Union*, *83*(40), 445. doi: 10.1029/2002EO000314

Schubert, M., Marcussen, T., Meseguer, A. S., & Fjellheim, S. (2019, May). The grass subfamily Pooideae: Cretaceous–Palaeocene origin and climate-driven Cenozoic diversification. *Global Ecology and Biogeography*(28). doi: 10.1111/geb.12923

Schwartz, T. M. (2015). *Insights into the growth and decay of orogenic wedges from foreland basin successions* (Unpublished doctoral dissertation). Stanford University, Stanford, CA.

Schwartz, T. M., Methner, K., Mulch, A., Graham, S. A., & Chamberlain, C. P. (2019, July). Paleogene topographic and climatic evolution of the Northern Rocky Mountains from integrated sedimentary and isotopic data. *GSA Bulletin*, *131*(7-8), 1203–1223. doi: 10.1130/B32068.1

Sewall, J. O., & Sloan, L. C. (2006). Come a little bit closer: A high-resolution climate study of the early Paleogene Laramide foreland. *Geology*, *34*(2), 81. doi: 10.1130/G22177.1

Sharp, Z. D. (1990). A laser-based microanalytical method for the in situ determination of oxygen isotope ratios of silicates and oxides. *Geochimica et Cosmochimica Acta*, *54*(5), 1353–1357. doi: 10.1016/0016-7037(90)90160-M

Sheppard, S., & Gilg, H. (1996). Stable isotope geochemistry of clay minerals. *Clay Minerals*, *31*, 1–24. doi: 10.1180/claymin.1996.031.1.01

Siler, N., & Durran, D. (2016). What Causes Weak Orographic Rain Shadows ? Insights from Case Studies in the Cascades and Idealized Simulations. *American Meteorological Society*, 4077–4099. doi: 10.1175/JAS-D-15-0371.1

Siler, N., Roe, G., & Durran, D. (2013). On the Dynamical Causes of Variability in the Rain-Shadow Effect: A Case Study of the Washington Cascades. *Journal of Hydrometeorology*, *14*(1), 122–139. doi: 10.1175/JHM-D-12-045.1

Sjostrom, D. J., Hren, M. T., Horton, T. W., Waldbauer, J. R., & Chamberlain, C. P. (2006). Stable isotopic evidence for a pre–late Miocene elevation gradient in the Great Plains–Rocky Mountain region, USA. *Geological Society of America Special Papers*, *398*(19), 309–319. doi: 10.1130/2006.2398(19).

Smiley, T. M., Hyland, E. G., Cotton, J. M., & Reynolds, R. E. (2018, January). Evidence of early C4 grasses, habitat heterogeneity, and faunal response during the Miocene Climatic Optimum in the Mojave Region. *Palaeogeography, Palaeoclimatology, Palaeoecology*, *490*, 415–430. doi: 10.1016/j.palaeo.2017.11.020

Stern, L. A., Chamberlain, C. P., Reynolds, R. C., & Johnson, G. D. (1997). Oxygen isotope evidence of climate change from pedogenic clay minerals in the Himalayan molasse. *Geochimica et Cosmochimica Acta*, *61*(4), 731–744. doi: 10.1016/S0016-7037(96)00367-5

Strömberg, C. A. E. (2005, August). Decoupled taxonomic radiation and ecological expansion of open-habitat grasses in the Cenozoic of North America. *Proceedings of the National Academy of Sciences*, *102*(34), 11980–11984. doi: 10.1073/pnas.0505700102

Strömberg, C. A. E. (2011). Evolution of Grasses and Grassland Ecosystems. *Annual Review of Earth and Planetary Sciences*, *39*(1), 517–544. doi: 10.1146/annurev-earth-040809-152402

Strömberg, C. A. E., Dunn, R. E., Crifò, C., & Harris, E. B. (2018). Phytoliths in Paleoecology: Analytical Considerations, Current Use, and Future Directions. In D. A. Croft, D. F. Su, & S. W. Simpson (Eds.), *Methods in Paleoecology* (pp. 235–287). Cham: Springer International Publishing. doi: 10.1007/978-3-319-94265-0_12

Strömberg, C. A. E., Dunn, R. E., Madden, R. H., Kohn, M. J., & Carlini, A. A. (2013, June). Decoupling the spread of grasslands from the evolution of grazer-type herbivores in South America. *Nature Communications*, *4*(1). doi: 10.1038/ncomms2508

Strömberg, C. A. E., & McInerney, F. A. (2011). The Neogene transition from C $_3$ to C $_4$ grasslands in North America: Assemblage analysis of fossil phytoliths. *Paleobiology*, *37*(1), 50–71. doi: 10.1666/09067.1

Swisher, C. C., & Prothero, D. R. (1990, August). Single-Crystal 40Ar/39Ar Dating of the Eocene-Oligocene Transition in North America. *Science*, *249*(4970), 760–762. doi: 10.1126/science.249.4970.760

Tabor, N. J., Montanez, I. P., & Southard, R. J. (2002, September). Paleoenvironmental reconstruction from chemical and isotopic compositions of Permo-Pennsylvanian pedogenic minerals. *Geochimica et Cosmochimica Acta*, *66*(17), 3093–3107. doi: 10.1016/S0016-7037(02)00879-7

Takeuchi, A. (2007). *Decoupling the Ancient Hydrologic System From the Modern Hydrologic System of Pacific Northwest in the United States: Implications for the Evolution of Topography, Climate, and Environment* (Unpublished doctoral dissertation). Washington State University.

Takeuchi, A., Hren, M. T., Smith, S. V., Chamberlain, C. P., & Larson, P. B. (2010). Pedogenic carbonate carbon isotopic constraints on paleoprecipitation: Evolution of desert in the Pacific Northwest, USA, in response to topographic development of the Cascade Range. *Chemical Geology*, *277*(3-4), 323–335. doi: 10.1016/j.chemgeo.2010.08.015

Takeuchi, A., & Larson, P. B. (2005). Oxygen isotope evidence for the late Cenozoic development of an orographic rain shadow in eastern Washington, USA. *Geology*, *33*(4), 313–316. doi: 10.1130/G21335.1

Terry, D. O., Jr. (2001, April). Paleopedology of the Chadron Formation of Northwestern Nebraska: Implications for paleoclimatic change in the North American midcontinent across the Eocene–Oligocene boundary. *Palaeogeography, Palaeoclimatology, Palaeoecology*, *168*(1-2), 1–38. doi: 10.1016/S0031-0182(00)00248-0

Torres-Ruíz, J., López-Galindo, A., González-López, J., & Delgado, A. (1994, February). Geochemistry of Spanish sepiolite-palygorskite deposits: Genetic considerations based on trace elements and isotopes. *Chemical Geology*, *112*(3-4), 221–245. doi: 10.1016/0009-2541(94)90026-4

Trujillo, E., Molotch, N. P., Goulden, M. L., Kelly, A. E., & Bales, R. C. (2012, October). Elevation-dependent influence of snow accumulation on forest greening. *Nature Geoscience*, *5*(10), 705–709. doi: 10.1038/ngeo1571

Webb, S. D., & Opdyke, N. D. (1995). *Effects of Past Global Change on Life.* Washington: National Academies Press.

Westerhold, T., Marwan, N., Drury, A. J., Liebrand, D., Agnini, C., Anagnostou, E., ... Zachos, J. C. (2020, September). An astronomically dated record of Earth's climate and its predictability over the last 66 million years. *Science*, *369*(6509), 1383–1387. doi: 10.1126/science.aba6853

Wheeler, E. A., Manchester, S. A., & Wiemann, M. (2006). Eocene woods of central Oregon. *PaleoBios*, *26*(3), 6.

White, A. F., Schulz, M. S., Vivit, D. V., Blum, A. E., Stonestrom, D. A., & Anderson, S. P. (2008, January). Chemical weathering of a marine terrace chronosequence, Santa Cruz, California I: Interpreting rates and controls based on soil concentration–depth profiles. *Geochimica et Cosmochimica Acta*, *72*(1), 36–68. doi: 10.1016/j.gca.2007.08.029

Wing, S. L. (1998). Tertiary vegetation of North America as a context for mammalian evolution. In C. M. Janis, K. M. Scott, & L. L. Jacobs (Eds.), *Evolution of Tertiary Mammals of North America* (Vol. 1, pp. 37–60). Cambridge University Press.

Winnick, M. J., Chamberlain, C. P., Caves, J. K., & Welker, J. M. (2014). Quantifying the isotopic 'continental effect'. *Earth and Planetary Science Letters*, *406*, 123–133. doi: 10.1016/j.epsl.2014.09.005

Wolfe, J. A. (1985). Distribution of Major Vegetational Types During the Tertiary. In E. Sundquist & W. Broecker (Eds.), *Geophysical Monograph Series* (pp. 357–375). Washington, D. C.: American Geophysical Union. doi: 10.1029/GM032p0357

Zachos, J., Pagani, M., Sloan, L., Thomas, E., & Billups, K. (2001). Trends, rhythms, and aberrations in global climate 65 Ma to present. *Science*, *292*(5517), 686–693. doi: 10.1126/science.1059412

Zanazzi, A., Kohn, M. J., MacFadden, B. J., & Terry, D. O. (2007). Large temperature drop across the Eocene-Oligocene transition in central North America. *Nature*, *445*(February), 639–642. doi: 10.1038/nature05551

Zimmermann, U., Ehhalt, D., & Münnich, K. (1967). Soil-water movement and evapotranspiration: Changes in the isotopic composition of the water. In *Isotopes and Hydrology* (pp. 567–586). Vienna, Austria: International Atomic Energy Agency.

Supporting Information for "Drier winters drove Cenozoic open habitat expansion in North America"

T. Kukla[1], J. K. C. Rugenstein[2], D. E. Ibarra[3,4], M. J. Winnick[5], C. A. E. Strömberg[6], C. P. Chamberlain[1]

[1]Department of Geological Sciences, Stanford University, Stanford, CA 94305

[2]Department of Geosciences, Colorado State University, Fort Collins 80521

[3]Institute at Brown for Environment and Society and the Department of Earth, Environmental and Planetary Science, Brown University, Providence, RI 02912

[4]Department of Earth and Planetary Science, University of California, Berkeley, Berkeley, CA 94709

[5]Department of Geosciences, University of Massachusetts, Amherst, Amherst, MA 01003

[6]Department of Biology & Burke Museum of Natural History and Culture, University of Washington, Seattle, WA 98195

Contents of this file

1. Text S1 to S4
2. Table S1
3. Figures S1 to S13

Additional Supporting Information (Files uploaded separately)

1. Isotope data
2. Phytolith data
3. Unprocessed/unfiltered initial isotope data (input to R script)

4. Isotoped data at each step of data processing (R script outputs)

5. R script to process isotope data and generate results

Introduction

The supporting information includes elaboration on some details in the main text (see Text S1-S4) and the supporting table and figures referenced in the main text (Table S1; Fig. S1-S13). Please see external data files for isotope and phytolith data to reproduce the figures in the text as well as an R script to conduct all of the isotope data processing and statistics.

Text S1: Clay and carbonate oxygen isotope difference in co-equilibrium

We use the clay and carbonate mineral temperature-dependent fractionation factors to define the solution space of differences in mineral formation temperatures and soil water $\delta^{18}O$. For carbonate (specifically calcite), we use the equation of Kim and O'Neil (1997):

$$1000ln\alpha_{calcite-water} = 18.03(10^3T^{-1}) - 32.42 \quad (1)$$

where α is the $^{18}O/^{16}O$ ratio of carbonate over the $^{18}O/^{16}O$ ratio of the water in which the carbonate forms and T is temperature in Kelvin.

For authigenic clay minerals, we use the smectite and kaolinite fractionation equations of Sheppard and Gilg (1996) where smectite is:

$$1000ln\alpha_{smectite-water} = 2.55(10^6T^{-2}) - 4.05 \quad (2)$$

and kaolinite is:

$$1000ln\alpha_{kaolinite-water} = 2.76(10^6T^{-2}) - 6.75. \quad (3)$$

The fractionation factor, α, is then related to the $\delta^{18}O$ of the mineral and water by

$$\alpha_{mineral-water} = \frac{1000 + \delta^{18}O_{mineral}}{1000 + \delta^{19}O_{water}}. \quad (4)$$

Reorganizing equation 4 shows that the difference in $\delta^{18}O$ between the mineral and water depends on the fractionation factor (α) and the water composition itself:

$$\delta^{18}O_{mineral} - \delta^{18}O_{water} = 1000(\alpha - 1) + \delta^{18}O_{water}(\alpha - 1). \quad (5)$$

A common, simplifying assumption allows us to re-write the mineral-water $\delta^{18}O$ difference solely as a function of the fractionation factor, α (and therefore temperature; see equations 1-3) by recognizing that the absolute value of $\delta^{18}O_{water} << 1000$ so the second term on the right side of equation 5 can be ignored. Finally, because α is close to 1 for oxygen isotope fractionation in clay and carbonate minerals at environmental temperatures, the following approximation can be made:

$$1000ln\alpha \approx 1000(\alpha - 1) \approx \delta^{18}O_{mineral} - \delta^{18}O_{water}. \quad (6)$$

The approximations that lead to equation 6 are important because they demonstrate that, if clay and carbonate minerals are forming in the same fluid at the same temperature (co-equilibrium), the difference between clay and carbonate $\delta^{18}O$ can be written as a single function of temperature. For example, from equation 6, the difference between clay and carbonate $\delta^{18}O$ can be written as:

$$\Delta\delta^{18}O_{clay-calcite} = 1000ln\alpha_{clay-water} - 1000ln\alpha_{calcite-water}. \quad (7)$$

Then, plugging in equations 1-3 gives the following equations for smectite and kaolinite

$$\Delta\delta^{18}O_{smectite-calcite} = 2.55(10^6T^{-2}) - 18.03(10^3T^{-1}) + 28.37 \quad (8)$$

$$\Delta\delta^{18}O_{kaolinite-calcite} = 2.76(10^6T^{-2}) - 18.03(10^3T^{-1}) + 25.67. \quad (9)$$

The simplification in equations 8 and 9 is useful for demonstrating that the difference between clay and carbonate $\delta^{18}O$ in co-equilibrium can be closely approximated with no prior knowledge of the $\delta^{18}O$ of water. Therefore, we can use the same co-equilibrium $\Delta\delta^{18}O$ for all domains in WCNA.

Importantly, the equilibrium $\Delta\delta^{18}O$ value is only weakly sensitive to temperature because the temperature-dependent fractionation slopes for clay and carbonate minerals are similar. For environmental temperatures, equations 8 and 9 give values near $-3.5‰$ with a maximum kaolinite-smectite difference of less than 0.5‰ (Fig. S3). Therefore, $-3.5‰$ can be considered the expected $\Delta\delta^{18}O_{clay-carb}$ when clay and carbonate minerals form in equilibrium with one another.

We quantify the error introduced by the approximations in equation 6 by calculating the equilibrium $\Delta\delta^{18}O$ for water $\delta^{18}O$ values ranging from $-30‰$ to $-5‰$ (conservative range in WCNA). We find that, within this range, the maximum error owed to the approximations is $< 0.1‰$ (Fig. S3).

Text S2: Carbonate formation in the western domain

Carbonate formation in the western domain differs from the central and eastern domains in that there is a lack of soil carbonates prior to 30 Ma. A notable exception to this comes from the Eocene/Oligocene Chumstick Basin in central Washington, where large ($>$ 10cm diameter) carbonate concretions and warm (60-130°C) clumped isotope and vitrinite reflectance derived temperatures provide strong evidence for groundwater carbonate formation (Methner et al., 2016). These measurements are excluded from our study's compilation due to the unusually high formation temperatures.

While clumped isotope measurements have not been conducted on the late Oligocene carbonates in the western domain, these carbonates share similar features with the Chumstick Basin concretions measured by (Methner et al., 2016). Specifically, the late Oligocene carbonates (from the John Day region of central Oregon, (Retallack et al., 2004; McLean & Bershaw, 2021)) form in distinct layers (Fig. S7a) and in concretions commonly exceeding 20cm diameter (Fig. S7b). The paleosols containing these carbonates are tan to green and considered poorly-drained, suggesting longer water residence times (Bestland et al., 2002).

Based on these observations, it is possible that the earliest western domain carbonates in our record formed in contact with groundwater that has a long enough residence time to preserve winter precipitation trends. If this is the case, both clays and carbonates may be influenced by winter precipitation in the late Oligocene/early Miocene. This scenario can explain why, with the exception of the oldest western domain $\delta^{18}O$ data point (from the John Day region; (McLean & Bershaw, 2021)), carbonate $\delta^{18}O$ appears to increase with clay $\delta^{18}O$ across the OHT (see Fig. 2 of the main text). Regardless, we find a robust increase in western domain $\Delta\delta^{18}O_{clay-carb}$ associated with the OHT. The possible influence of groundwater (dominated by winter precipitation (Jasechko et al., 2014)) on carbonate formation would act to dampen this $\Delta\delta^{18}O_{clay-carb}$ increase, suggesting that, if anything, our results underestimate the magnitude of winter drying in the western domain. Elevated carbonate formation temperatures, similar to the Chumstick Basin (Methner et al., 2016) would further dampen the signal by increasing $\Delta\delta^{18}O_{clay-carb}$ (decreasing carbonate $\delta^{18}O$) before the OHT.

Text S3: The oxygen isotope response to a proposed pre-OHT Oregon "monsoon" climate

A shift from a summer wet "monsoon" climate to the modern, winter-wet "Mediteranean" climate in Oregon has previously been argued as a driver of open habitat expansion (Retallack, 2004). Here, we expand on why this scenario cannot be reconciled with our results.

Assuming that summer was the low-$\delta^{18}O_p$ season before the OHT due to a monsoonal climate, the shift to a winter-wet climate would correspond with the onset of low-$\delta^{18}O_p$ winters. The clay oxygen isotope composition during this shift would primarily depend on two factors: (1) the change in the fractional contribution of summer versus winter precipitation and (2) the change in $\delta^{18}O_p$ during the wet (low-$\delta^{18}O_p$) season. In order for clay $\delta^{18}O$ to increase across the OHT, winters after the OHT would have to be drier than summers before the OHT such that the low-$\delta^{18}O_p$ season has a lower contribution to annual precipitation. This scenario is unlikely because it requires summer precipitation to significantly outpace the wintertime westerlies which have been active for at least the last 50 million years (Norris et al., 1996; Feng et al., 2013; Morrill & Koch, 2002; Sewall & Sloan, 2006). We are not aware of climate modeling evidence for summertime precipitation outpacing winter in warmer climates of the Pacific Northwest. Additionally, wet season $\delta^{18}O_p$ must stay the same (if the wet season contributes less to annual precipitation after the OHT) or increase (if the wet season contributes as as much or more) in order for clay $\delta^{18}O$ to increase. However, since the Cascades present a stronger winter rainshadow than summer, a winter-wet climate would likely amplify the $\delta^{18}O_p$ decrease in east-central Oregon compared to summer, leading to a decrease in clay $\delta^{18}O$.

Further, carbonate $\delta^{18}O$ would probably increase in this scenario due to a summer-wet to winter-wet transition. This is mostly inconsistent with our results, although a statistically significant increase in carbonate $\delta^{18}O$ emerges using all data (the shift is not significant with the site averaged data). In a summer-wet (winter-wet) climate, soil carbonates are likely to form in the spring/fall (summer) (Breecker et al., 2009; Peters et al., 2013; Kelson et al., 2020; Huth et al., 2019; Gallagher & Sheldon, 2016). If summer became the high-$\delta^{18}O_p$ dry season after the OHT, carbonate $\delta^{18}O$ would likely capture this increase. Fall $\delta^{18}O_p$ is lower than summer $\delta^{18}O_p$ today (Fig. 1b of the main text) and would likely have been lower than modern summer $\delta^{18}O_p$ in the past. Due to the warm-season bias associated with soil carbonates, we expect a signal of summer drying and the demise of a summer-wet climate would have a larger impact on carbonate $\delta^{18}O$ than clay $\delta^{18}O$. While western domain carbonates appear to increase across the OHT, this shift is likely due to carbonates tracking precipitation-weighted mean $\delta^{18}O$ (as preserved in groundwater; see Supplemental Text S1). We expect groundwater carbonates recording the demise of a summer-wet climate to record the same $\delta^{18}O$ signal as the authigenic clays, discussed above.

In addition to the lack of modeling evidence for a summer-wet climate in Oregon before the OHT, competing factors between summer and winter precipitation amounts and $\delta^{18}O_p$ make it highly unlikely that our results can be explained by a summer-wet to winter-wet transition. As discussed above, this conclusion holds even when we do not assume that winter has been the low-$\delta^{18}O_p$ season since the Paleogene (Norris et al., 1996; Feng et al., 2013; Morrill & Koch, 2002).

Text S4: Linear mixing model for oxygen isotope seasonality

An increase in clay $\delta^{18}O$ to the east of the Cascades is incompatible with uplift if the traditional rainout effect is the main $\delta^{18}O$ driver. However, as noted in the main text, east of the Cascades, uplift would increase the fraction of summertime (high-$\delta^{18}O$) precipitation (Fig 1d of the main text). We explore the trade-off between these effects—the uplift effect (decreasing $\delta^{18}O$) and the seasonality effect (increasing $\delta^{18}O$) with a two end-member mixing model.

We take winter (DJF_p) and summer (JJA_p) precipitation as isotopic end-members to estimate the precipitation-weighted $\delta^{18}O$ ($\delta^{18}O_{precip,ann}$) based on the following equation:

$$\delta^{18}O_{p,ann} = DJF_p\delta^{18}O_{p,DJF} + (1 - DJF_p)\delta^{18}O_{p,JJA}. \tag{10}$$

We apply uniform distributions to each of the inputs (DJF_p, $\delta^{18}O_{p,DJF}$, and $\delta^{18}O_{p,JJA}$) before and after the OHT ("pre and post uplift") and subsample from these inputs 50,000 times to build a solution space of possible outcomes. We assume the pre-uplift winter precipitation fraction in the western domain is the same as west of the Cascades today [0.75-1] and post uplift is the same as the western domain today [0.5-0.75]. The oxygen isotope range of winter and summer precipitation ($\delta^{18}O_{p,DJF}$ and $\delta^{18}O_{p,JJA}$) is the same before and after the OHT, meant to capture the cumulative range of both intervals: $\delta^{18}O_{p,DJF}$ is [-20, -6] and $\delta^{18}O_{p,JJA}$ is [-9, -6], based on monthly mean precipitation $\delta^{18}O$ (Fig. 1b of main text).

Based on the 50,000 iterations we calculate a convex hull to denote the solution space where the combination of the decrease in DJF $\delta^{18}O$ (the uplift effect) and the decrease in DJF precipitation fraction (the seasonality effect) yields an increase in precipitation-weighted $\delta^{18}O$ of more than 2‰ and less than 4‰ (Fig. S12). This marks a solution space consistent with the $\delta^{18}O$ increase observed in our results. The magenta polygon shows the range of possible solutions where wintertime $\delta^{18}O_p$ decreases while precipitation-weighted $\delta^{18}O_p$ increases due to the seasonality effect on $\delta^{18}O_p$ outpacing the uplift effect. Consistent with expectations, the seasonality effect must increase (a larger decrease in the DJF precipitation fraction) to outpace the uplift effect, as evidenced by the lack of solutions below zero on the y-axis when the x-axis exceeds ~ -0.1.

This analysis treats the change in DJF $\delta^{18}O_p$ and the change in the DJF precipitation fraction as independent but, in reality, they are positively related when uplift provides a stronger winter rainshadow compared to summer. For example, a decrease in DJF $\delta^{18}O_p$ with uplift occurs due to more windward rainout which implies a decrease in leeward DJF precipitation. If the fractional loss of summer precipitation is the same as the fractional loss in winter, uplift will cause a decrease in the y-axis (lower DJF $\delta^{18}O_p$) with no change in the x-axis (the fraction of winter precipitation) (downward arrow in Fig. S12). In contrast, if the fractional loss of summer precipitation is smaller than winter, (*i.e.* if the winter rainshadow is stronger) then uplift will cause a decrease in winter $\delta^{18}O_p$ and in the winter precipitation fraction (diagonal arrow in Fig. S12). Put otherwise, the sharp gradient in precipitation seasonality across the Cascades Range today (Fig. 1d of the main text) is evidence that uplift would have caused the east side of the Cascades to move down and to the left in Figure S12. The slope of this shift would depend on the strength of the winter rainshadow relative to summer (which, itself, may be a function of uplift (Siler & Durran, 2016)).

While the mixing model analysis identifies that an increase in clay $\delta^{18}O$ with Cascades uplift is plausible, it does not confirm that uplift caused drier winters across the OHT. Factors that decrease westerly precipitation without varying the height of the Cascades, like weaker westerly transport or a latitudinal shift of the jet stream, could also explain our results and should be explored. Such analysis, however, is outside the scope of this work.

References

Berkelhammer, M., Still, C. J., Ritter, F., Winnick, M., Anderson, L., Carroll, R., ... Williams, K. H. (2020, February). Persistence and Plasticity in Conifer Water-Use Strategies. *Journal of Geophysical Research: Biogeosciences*, *125*(2). doi: 10.1029/2018JG004845

Bestland, E. A., Hammond, P. E., Blackwell, D. L. S., Kays, M. A., Retallack, G. J., & Stimac, J. (2002). Geologic Framework of the Clarno Unit, John Day Fossil Beds National Monument, Central Oregon. *Oregon Department of Geology and Mineral Industries Open-File Report*, 1–39.

Breecker, D., Sharp, Z., & McFadden, L. (2009, March). Seasonal bias in the formation and stable isotopic composition of pedogenic carbonate in modern soils from central New Mexico, USA. *Geological Society of America Bulletin*, *121*(3-4), 630–640. doi: 10.1130/B26413.1

Cluett, A. A., Thomas, E. K., Evans, S. M., & Keys, P. W. (2021, June). Seasonal Variations in Moisture Origin Explain Spatial Contrast in Precipitation Isotope Seasonality on Coastal Western Greenland. *Journal of Geophysical Research: Atmospheres*, *126*(11). doi: 10.1029/2020JD033543

Database, W. (2019). Retrieved from http://waterisotopes.org. Accessed 7/13/2019. Query: NLat=51, SLat=38, ELon=-90, WLon=-130, Type=Precipitation.

Feng, R., Poulsen, C. J., Werner, M., Chamberlain, C. P., Mix, H. T., & Mulch, A. (2013, September). Early Cenozoic evolution of topography, climate, and stable isotopes in precipitation in the North American Cordillera. *American Journal of Science*, *313*(7), 613–648. doi: 10.2475/07.2013.01

Gallagher, T. M., & Sheldon, N. D. (2016, October). Combining soil water balance and clumped isotopes to understand the nature and timing of pedogenic carbonate formation. *Chemical Geology*, *435*, 79–91. doi: 10.1016/j.chemgeo.2016.04.023

Geospatial Information Authority of Japan, Chiba University, & Collaborating Organizations. (2016). Vegetation (Percent Tree Cover) - Global Version - Version 1. *Globalmaps*.

Hollister, J., Shah, T., Robitaille, A. L., Beck, M. W., & Johnson, M. (2021). *Elevatr: Access Elevation Data from Various APIs.*

Hough, B. G., Fan, M., & Passey, B. H. (2014, April). Calibration of the clumped isotope geothermometer in soil carbonate in Wyoming and Nebraska, USA: Implications for paleoelevation and paleoclimate reconstruction. *Earth and Planetary Science Letters*, *391*, 110–120. doi: 10.1016/j.epsl.2014.01.008

Huth, T. E., Cerling, T. E., Marchetti, D. W., Bowling, D. R., Ellwein, A. L., & Passey, B. H. (2019, March). Seasonal Bias in Soil Carbonate Formation and Its Implications for Interpreting High-Resolution Paleoarchives: Evidence From Southern Utah. *Journal of Geophysical Research: Biogeosciences*, *124*(3), 616–632. doi: 10.1029/2018JG004496

Jasechko, S., Birks, S. J., Gleeson, T., Wada, Y., Fawcett, P. J., Sharp, Z. D., ... Welker, J. M. (2014, November). The pronounced seasonality of global groundwater recharge. *Water Resources Research*, *50*(11), 8845–8867. doi: 10.1002/2014WR015809

Kelson, J. R., Huntington, K. W., Breecker, D. O., Burgener, L. K., Gallagher, T. M., Hoke, G. D., & Petersen, S. V. (2020, April). A proxy for all seasons? A synthesis of clumped isotope data from Holocene soil carbonates. *Quaternary Science Reviews*, *234*, 106259. doi: 10.1016/j.quascirev.2020.106259

Keys, P. W., Barnes, E. A., van der Ent, R. J., & Gordon, L. J. (2014, October). Variability of moisture recycling using a precipitationshed framework. *Hydrology and Earth System Sciences*, *18*(10), 3937–3950. doi: 10.5194/hess-18-3937-2014

Kim, S.-T., & O'Neil, J. R. (1997). Equilibrium and nonequilibrium oxygen isotope effects in synthetic carbonates. *Geochimica et Cosmochimica Acta*, *61*(16), 3461–3475. doi: 10.1016/S0016-7037(97)00169-5

McLean, A., & Bershaw, J. (2021, March). Molecules to Mountains: A Multi-Proxy Investigation Into Ancient Climate and Topography of the Pacific Northwest, USA. *Frontiers in Earth Science*, *9*, 624961. doi: 10.3389/feart.2021.624961

Methner, K., Fiebig, J., Wacker, U., Umhoefer, P., Chamberlain, C. P., & Mulch, A. (2016). Eocene-Oligocene proto-Cascades topography revealed by clumped (Δ47) and oxygen isotope (δ18O) geochemistry (Chumstick Basin, WA, USA). *Tectonics*, *35*(3), 546–564. doi: 10.1002/2015TC003984

Morrill, C., & Koch, P. L. (2002). Elevation or alteration? Evaluation of isotopic constraints on paleoaltitudes surrounding the Eocene Green River Basin. *Geology*, *30*(4), 151–154.

Norris, R. D., Jones, L. S., Corfield, R. M., & Cartlidge, J. E. (1996). Skiing in the Eocene Uinta Mountains? Isotopic evidence in the Green River Formation for snow melt and large mountains. *Geology*, *24*(5), 403–406.

Passey, B. H., Levin, N. E., Cerling, T. E., Brown, F. H., & Eiler, J. M. (2010, June). High-temperature environments of human evolution in East Africa based on bond ordering in paleosol carbonates. *Proceedings of the National Academy of Sciences*, *107*(25), 11245–11249. doi: 10.1073/pnas.1001824107

Peters, N. A., Huntington, K. W., & Hoke, G. D. (2013, January). Hot or not? Impact of seasonally variable soil carbonate formation on paleotemperature and O-isotope records from clumped isotope thermometry. *Earth and Planetary Science Letters*, *361*, 208–218. doi: 10.1016/j.epsl.2012.10.024

PRISM, C. G. (2012). PRISM Climate Group, Oregon State University, http://prism.oregonstate.edu, created 20 Jul 2012. Accessed 3 Sep. 2020.

Quade, J., Eiler, J., Daëron, M., & Achyuthan, H. (2013, March). The clumped isotope geothermometer in soil and paleosol carbonate. *Geochimica et Cosmochimica Acta*, *105*, 92–107. doi: 10.1016/j.gca.2012.11.031

Retallack, G. J. (2004, May). Late Oligocene bunch grassland and early Miocene sod grassland paleosols from central Oregon, USA. *Palaeogeography, Palaeoclimatology, Palaeoecology*, *207*(3-4), 203–237. doi: 10.1016/j.palaeo.2003.09.027

Retallack, G. J., Wynn, J. G., & Fremd, T. J. (2004). Glacial-interglacial-scale paleoclimatic change without large ice sheets in the Oligocene of central Oregon. *Geology*, *32*(4), 297–300. doi: 10.1130/G20247.1

Sewall, J. O., & Sloan, L. C. (2006). Come a little bit closer: A high-resolution climate study of the early Paleogene Laramide foreland. *Geology*, *34*(2), 81. doi: 10.1130/G22177.1

Sheppard, S., & Gilg, H. (1996). Stable isotope geochemistry of clay minerals. *Clay Minerals*, *31*, 1–24. doi: 10.1180/claymin.1996.031.1.01

Siler, N., & Durran, D. (2016). What Causes Weak Orographic Rain Shadows ? Insights from Case Studies in the Cascades and Idealized Simulations. *American Meteorological Society*, 4077–4099. doi: 10.1175/JAS-D-15-0371.1

Tuinenburg, O. A., Theeuwen, J. J. E., & Staal, A. (2020, December). High-resolution global atmospheric moisture connections from evaporation to precipitation. *Earth System Science Data*, *12*(4), 3177–3188. doi: 10.5194/essd-12-3177-2020

Table S1. T-test results comparing pre and post-OHT $\delta^{18}O$ by mineral and domain. (Values are for all data. Significance also requires low p-values for site averages.)

	Domain	**Post- minus pre-OHT (‰)**	**Significant (p <0.05)**
Clay	**West**	**3.9**	**Y**
	Central	**2.7**	**Y**
	East	**0.8**	**Y**
Carbonate	West	2.3	N
	Central	-0.6	N
	East	**-1.9**	**Y**

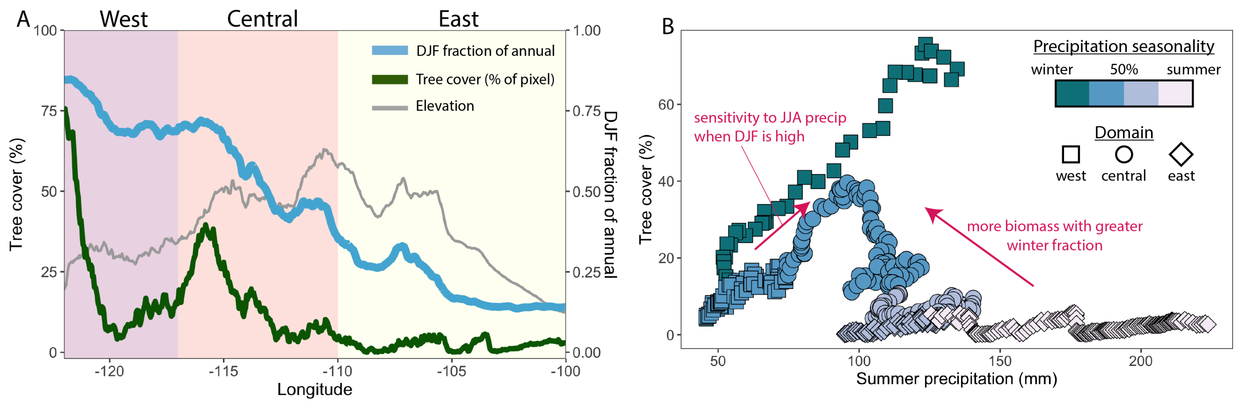

Figure S1. WCNA-averaged precipitation and tree cover from the leeward (eastward) side of the Cascades to the Great Plains. (**A**) Tree cover (percent of pixel) (Geospatial Information Authority of Japan et al., 2016) (green, left axis), fraction of DJF precipitation (PRISM, 2012) (blue, right axis) and elevation (Hollister et al., 2021) (gray). Peak tree cover and DJF precipitation decrease west-to-east with secondary peaks associated with high topography. (**B**) Tree cover percent generally decreases with summer precipitation amount and increases with the DJF fraction (northwest-facing arrow). The sensitivity of tree cover to summer precipitation increases with the DJF fraction as evidenced by intervals of positive-slope points (*e.g.* Berkelhammer et al. (2020)).

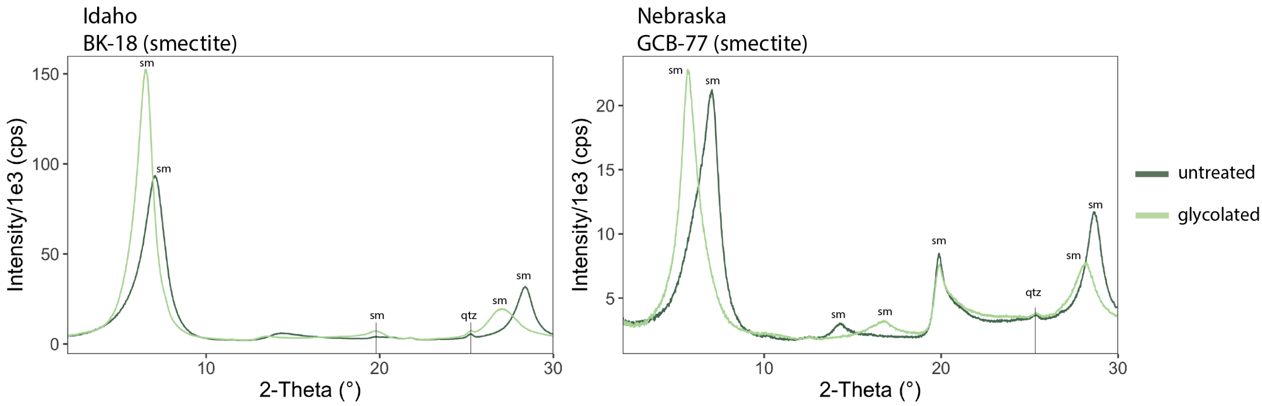

Figure S2. Characteristic XRD results for clay samples. Smectite peaks labeled with "sm" and quartz with "qtz". Minor quartz peaks indicate that isotopic contributions of quartz grains are likely negligible. Shifted peaks in the glycolated samples are characteristic of smectites (2:1 clays). Differences in relative peak heights between the Idaho and Nebraska samples may be owed to different compositions of smectite group minerals. All new clay data presented in this study come from smectite-dominant samples.

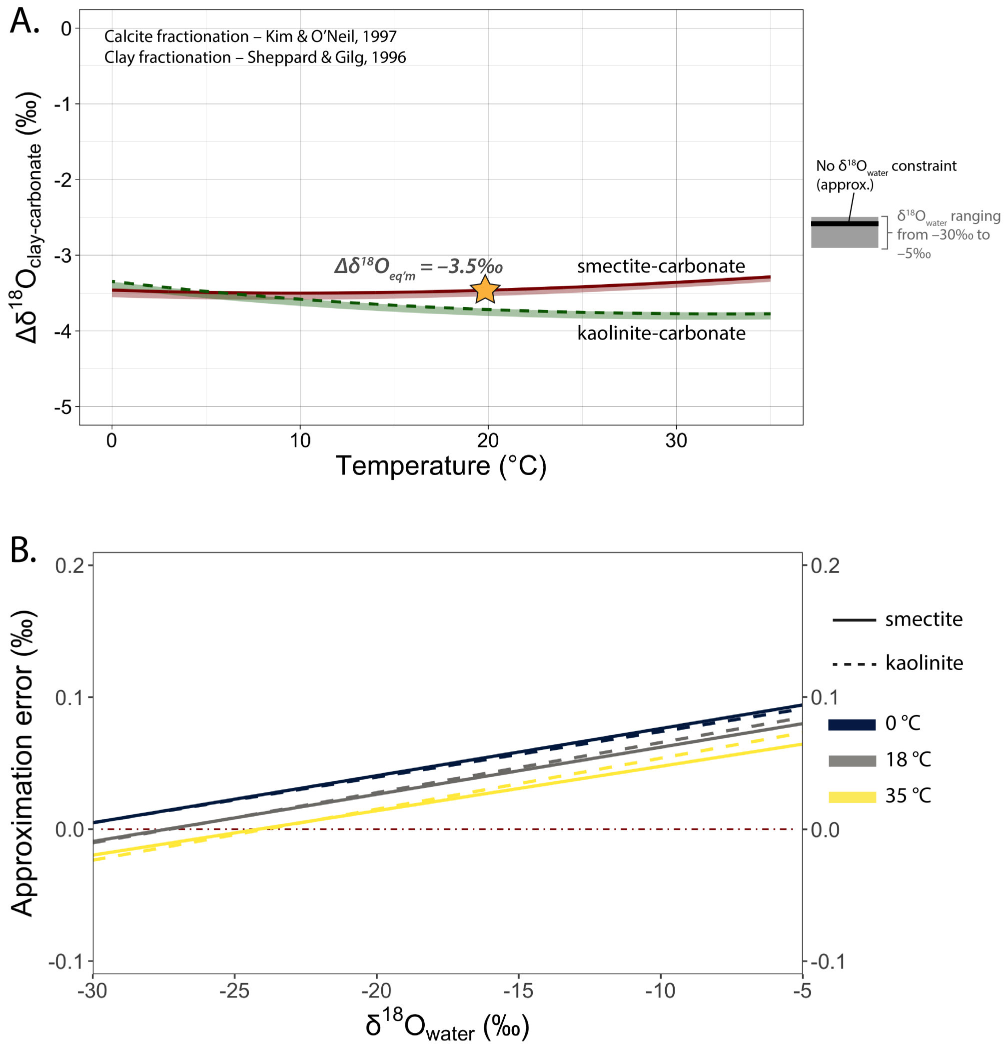

Figure S3. Calculating equilibrium $\Delta\delta^{18}O_{clay-carb}$ and error evaluation. (**A**) The difference between clay and carbonate $\delta^{18}O$ when minerals form at the same temperature and water $\delta^{18}O$. Solid lines are calculated from equations 8 and 9 in SI text 1 and shaded ribbons show the range of equilibrium $\Delta\delta^{18}O_{clay-carb}$ when we account for variation in WCNA water $\delta^{18}O$. Gold star denotes the equilibrium $\Delta\delta^{18}O_{clay-carb}$ used in this paper. (**B**) The error introduced by the approximations outlined in SI text (approximated $\Delta\delta^{18}O_{clay-carb}$ minus actual $\Delta\delta^{18}O_{clay-carb}$) for smectite-carbonate and kaolinite-carbonate (solid and dashed lines) at three different temperatures. Red dot-dashed line denotes zero error.

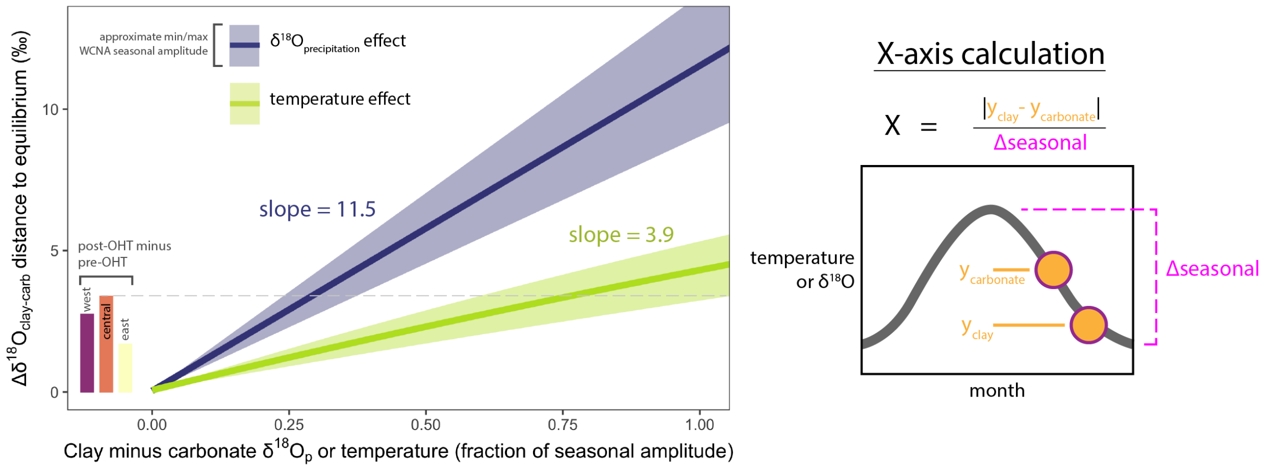

Figure S4. Comparing the sensitivity of $\Delta\delta^{18}O_{clay-carb}$ to changes in seasonality of temperature and precipitation $\delta^{18}O$. X-axis is the change in temperature (green line/ribbon) or $\delta^{18}O$ (purple line/ribbon) divided by the seasonal amplitude. Ribbon denotes the approximate min and max seasonal amplitudes across WCNA. Steeper slope of the purple line indicates $\Delta\delta^{18}O_{clay-carb}$ is more sensitive to the same fractional change in $\delta^{18}O_p$. A schematic outlining the X-axis calculation is shown on the right.

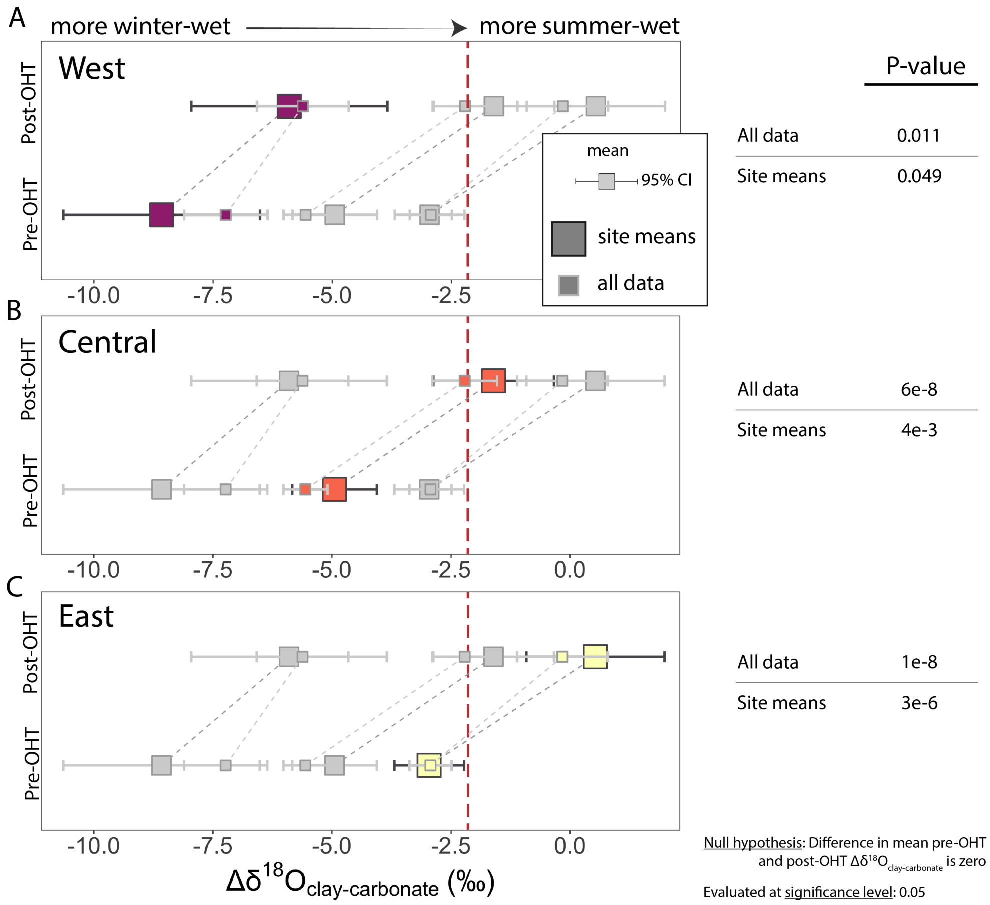

Figure S5. Comparison of $\Delta\delta^{18}O_{clay-carb}$ results before and after the OHT in each domain using all data (small squares) versus site averaged $\delta^{18}O$ (large squares) for the (**A**) west, (**B**) central, and (**C**) east domains. Averaging by site makes the data more sparse and increases the confidence intervals, however $\Delta\delta^{18}O_{clay-carb}$ increases significantly (p $<$ 0.05) in all domains. The magnitude of increase is similar in each domain suggesting the magnitude of the "all data" is not strongly biased by densely sampled sites.

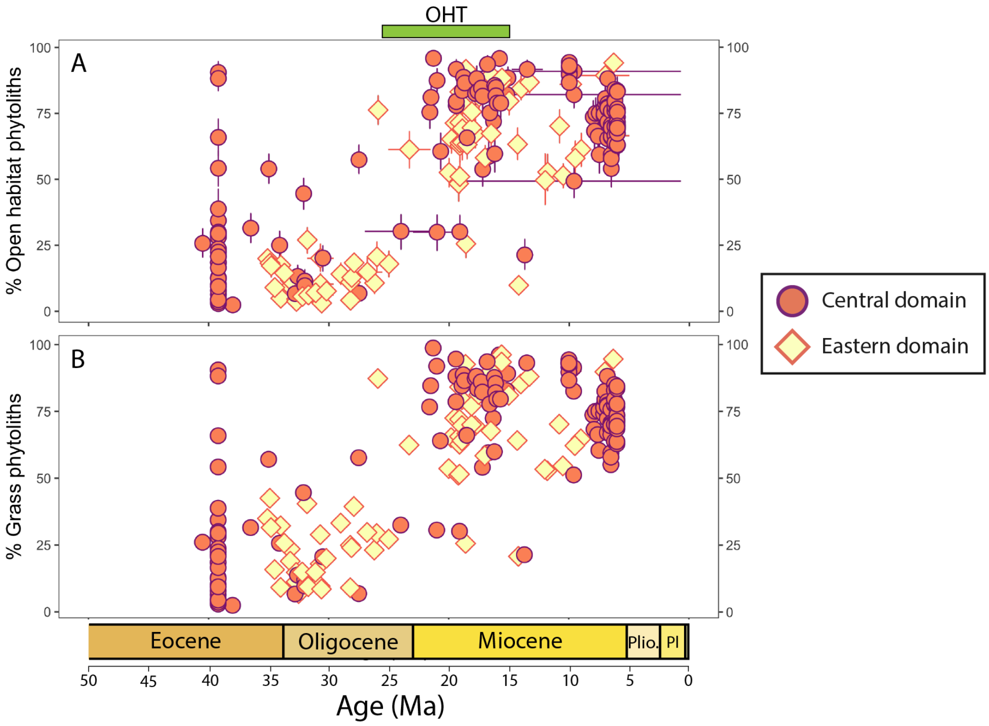

Figure S6. Percent of open habitat phytoliths (as in main text) (**A**) and grass phytoliths (**B**)

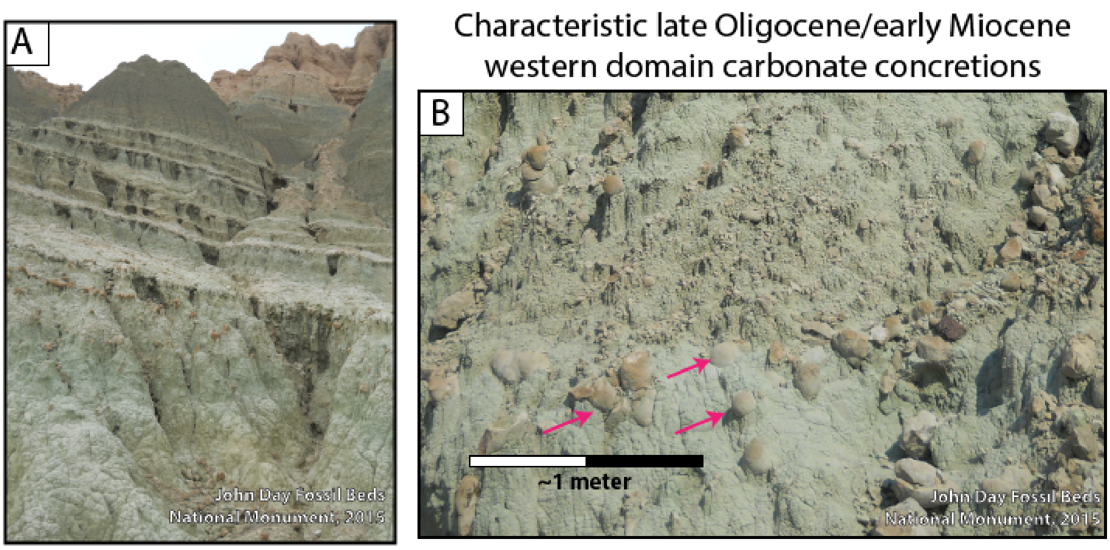

Figure S7. Pedogenic carbonates found in the late Oligocene/early Miocene of Oregon (western domain) show features consistent with groundwater carbonates found in the Eocene/Oligocene of Washington (Methner et al., 2016) including (**A**) well-defined horizontal layers and (**B**) large (> 10cm) concretions. Photos taken at John Day Fossil Beds National Monument in 2015.

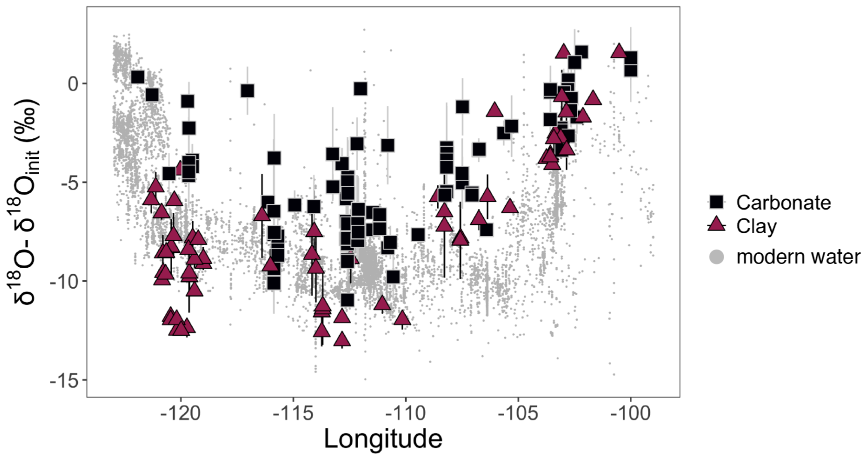

Figure S8. Oxygen isotope data from proxies (authigenic clay=orange circles; soil carbonate=purple circles) and modern water. All modern and proxy data are scaled so the "initial" (westernmost) value is approximately zero for comparison. Spatial pattern of modern water is in good agreement with the proxy data. Modern water data are river, stream, and groundwater measurements from the waterisotope database (accessed July 13, 2019) (Database, 2019).

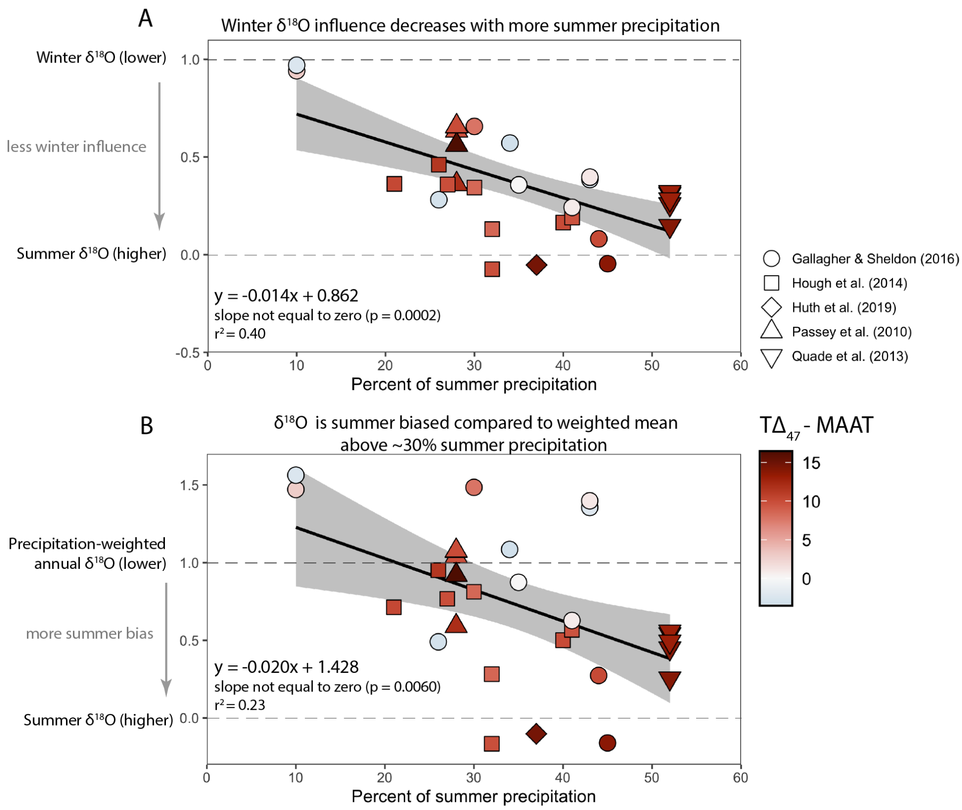

Figure S9. Late Quaternary soil carbonate $\delta^{18}O$ generally approaches summer precipitation $\delta^{18}O$ values as the percent of summer precipitation increases. Y-axis shows the distance of a given data point between two end-member $\delta^{18}O$ values that are scaled to 0-1 for comparison between sites. Data are from the western United States sites from Table S1 of Kelson et al. (2020) (Passey et al., 2010; Quade et al., 2013; Hough et al., 2014; Gallagher & Sheldon, 2016; Huth et al., 2019), (**A**) The influence of winter precipitation on carbonate $\delta^{18}O$ appears to decrease with a greater fraction of summer precipitation and (**B**) relative to precipitation-weighted $\delta^{18}O$, soil carbonates show a summer-bias in $\delta^{18}O$ as the percent of summer precipitation exceeds ~20-30%. Color bar shows that clumped isotope-derived temperatures are warmer than mean annual temperatures in almost all cases (except some data of Gallagher and Sheldon (2016)), consistent with a warm season formation bias (spring, summer, fall).

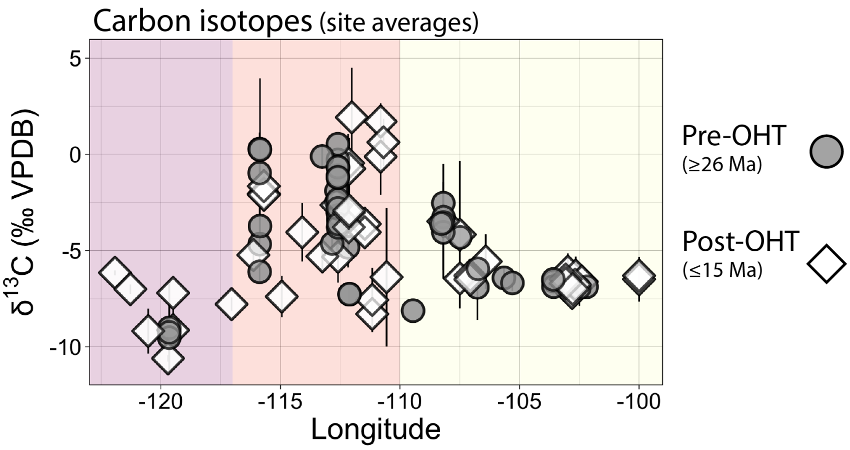

Figure S10. Site averaged carbon isotope ratios over longitude before (grey circles) and after (white diamonds) the OHT. We do not find any statistically significant change in $\delta^{13}C$ across the OHT.

		25% change in DJF precipitation fraction	Average of the three domains	Range of the three domains
Change in $\Delta\delta^{18}O$	All data	2.4‰	2.6‰	1.6 - 3.3 ‰
	Site means	2.8‰	3.2‰	2.7 - 3.5 ‰

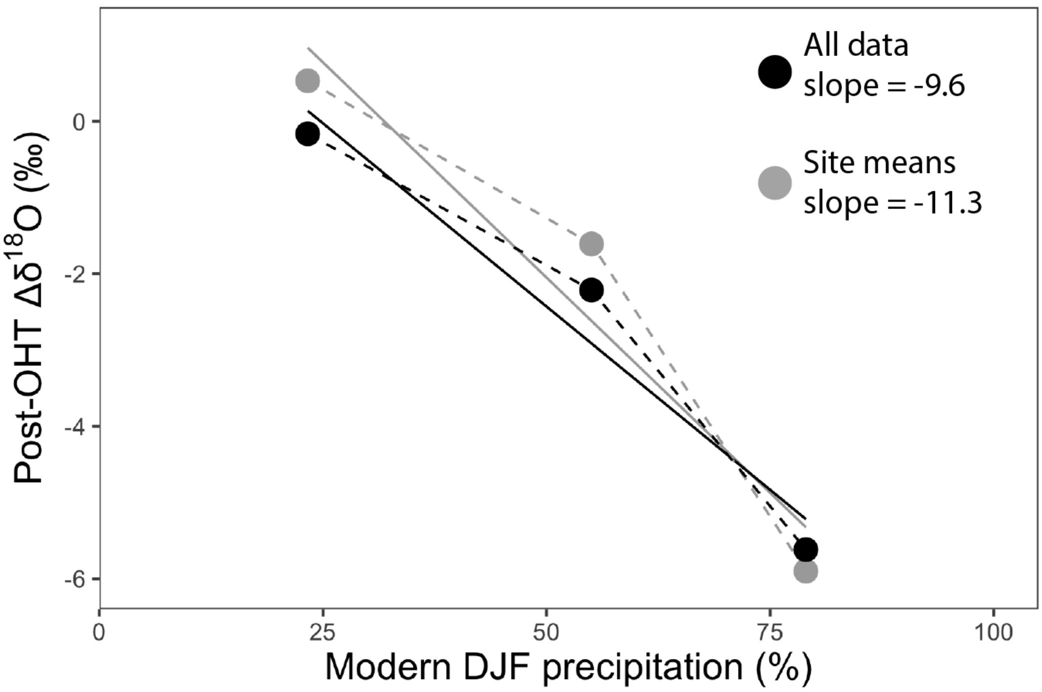

Figure S11. **Top** Table showing the increase in $\Delta\delta^{18}O_{clay-carb}$ consistent with a 25% decrease in DJF precipitation based on the regressions below. The range and average of increases in $\Delta\delta^{18}O_{clay-carb}$ using all data and site means are consistent with a 25% decrease in DJF precipitation for each respective regression. (**Bottom**) Post-OHT $\Delta\delta^{18}O_{clay-carb}$ data (the average value for each domain) plotted against the average modern DJF precipitation % for each domain. The slope of the $\Delta\delta^{18}O_{clay-carb}$-DJF precipitation relationship over space is used to develop a crude estimate for the change in DJF precipitation across the OHT.

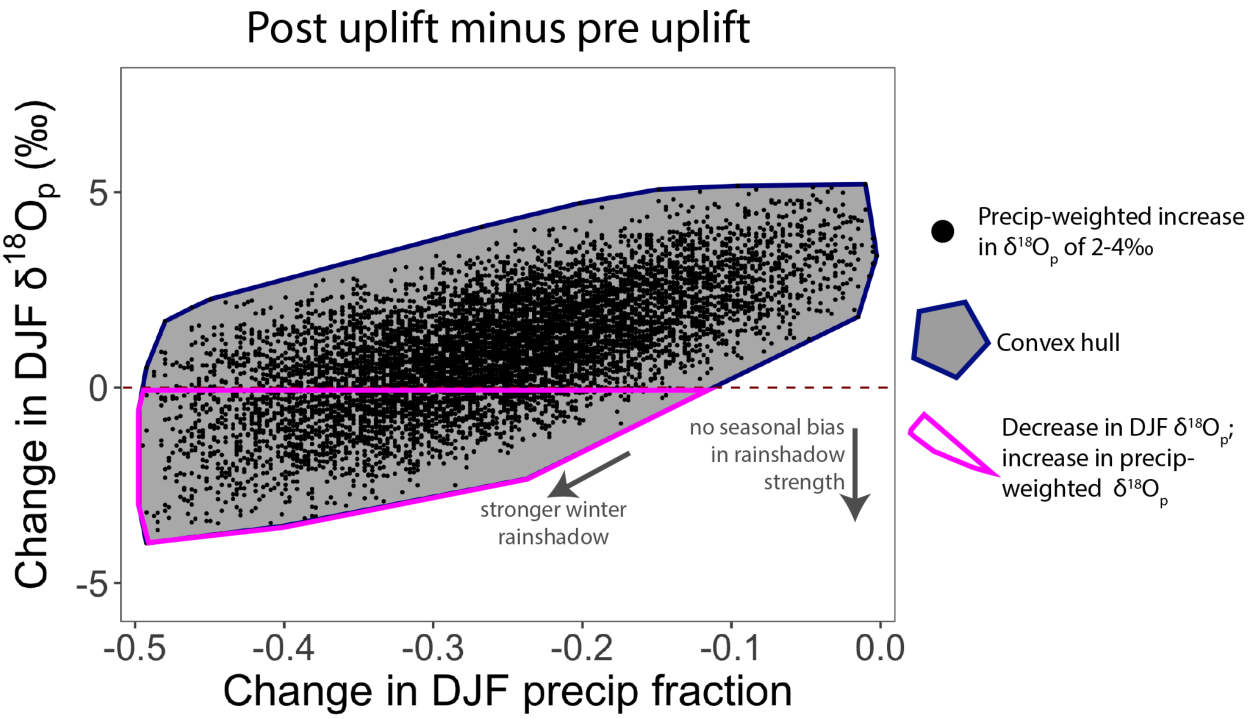

Figure S12. Linear two end-member mixing model results for precipitation and $\delta^{18}O_p$ seasonality (Supplemental Text S3). The x-axis and y-axis refer to the "seasonality effect" and "uplift effect" of the main text. Gray polygon is a convex hull for all results where precipitation-weighted $\delta^{18}O$ increases by 2-5‰ (consistent with the clay $\delta^{18}O$ signal). Magenta polygon shows range of solutions where DJF $\delta^{18}O_p$ decreases (*e.g.* due to uplift) while precipitation-weighted $\delta^{18}O_p$ increases (*e.g.* due to the change in precipitation seasonality). Because the Cascades Range is a stronger winter rainshadow, the east of the Cascades will move down and to the left (diagonal arrow) with uplift.

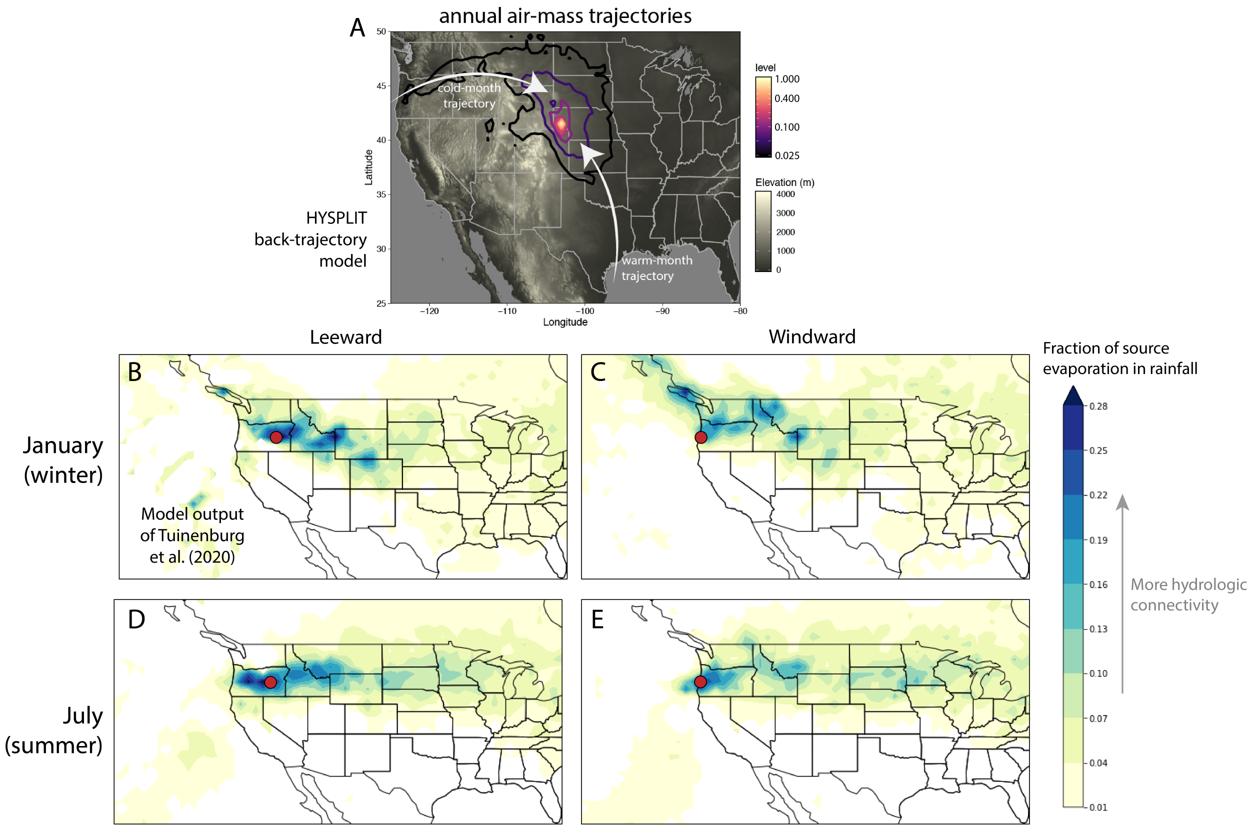

Figure S13. Hydrologic connections between the Cascades (western domain) and the Great Plains (eastern domain). (**A**) HYSPLIT back-trajectory modeling reveals precipitation in western Nebraska is derived from two main moisture sources—a Gulf source (the Great Plains Low Level Jet) that is dominant in summer, and a Pacific source (the westerlies) dominant in winter (Arctic air masses will follow the westerly source, although generally east of the Cascades). (**B-E**) Maps of the hydrologic connections between evaporation from a given source (red dots) and precipitation elsewhere (colored pixels) using evaporation moisture tracking data from Tuinenburg et al. (2020). This evaporation-downstream rainout link is commonly used as a metric for the hydrologic connection between two places (Keys et al., 2014; Cluett et al., 2021). Maps show that a substantial fraction of moisture sourced from the east (leeward) and west (windward) of the Cascades (red dots denote moisture source) reaches the Great Plains today. We expect that this moisture contribution would be higher in the past with a lower Cascades Range in the past.